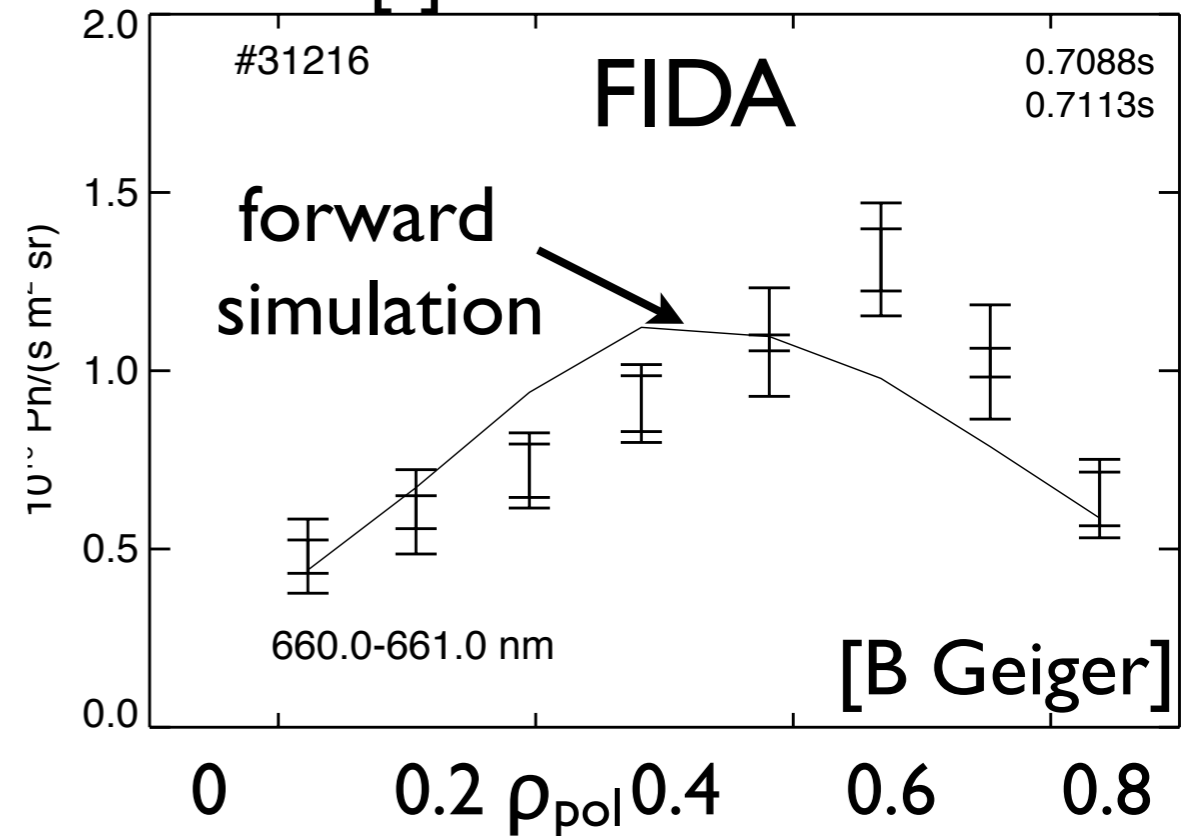
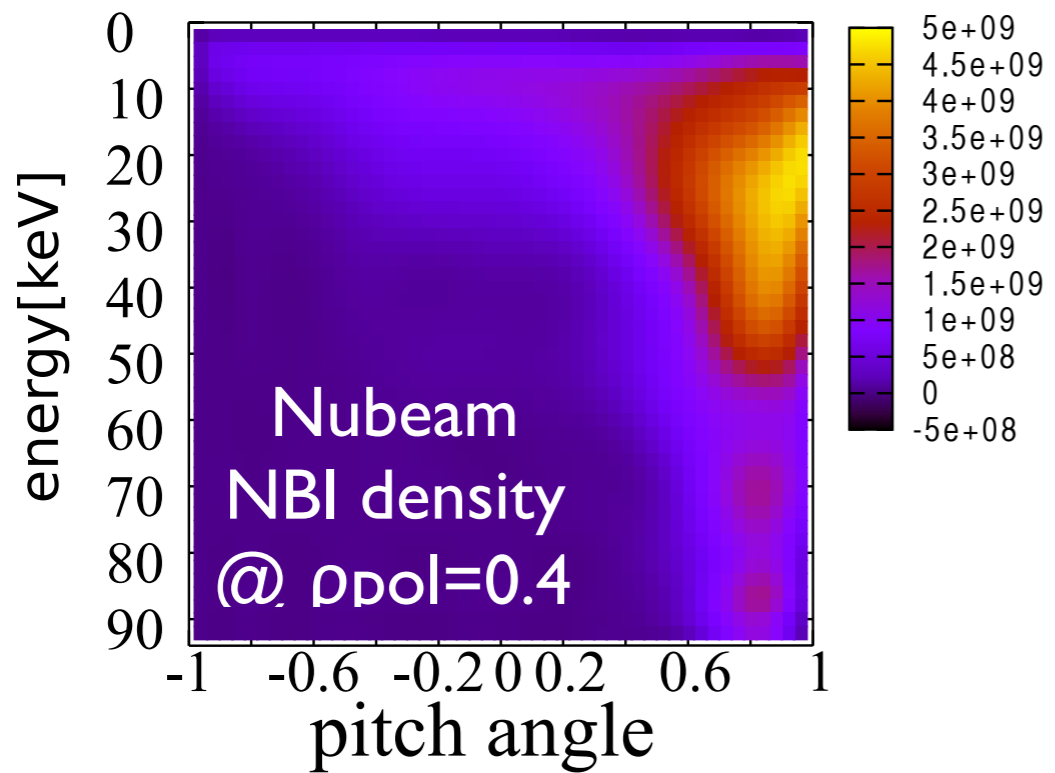
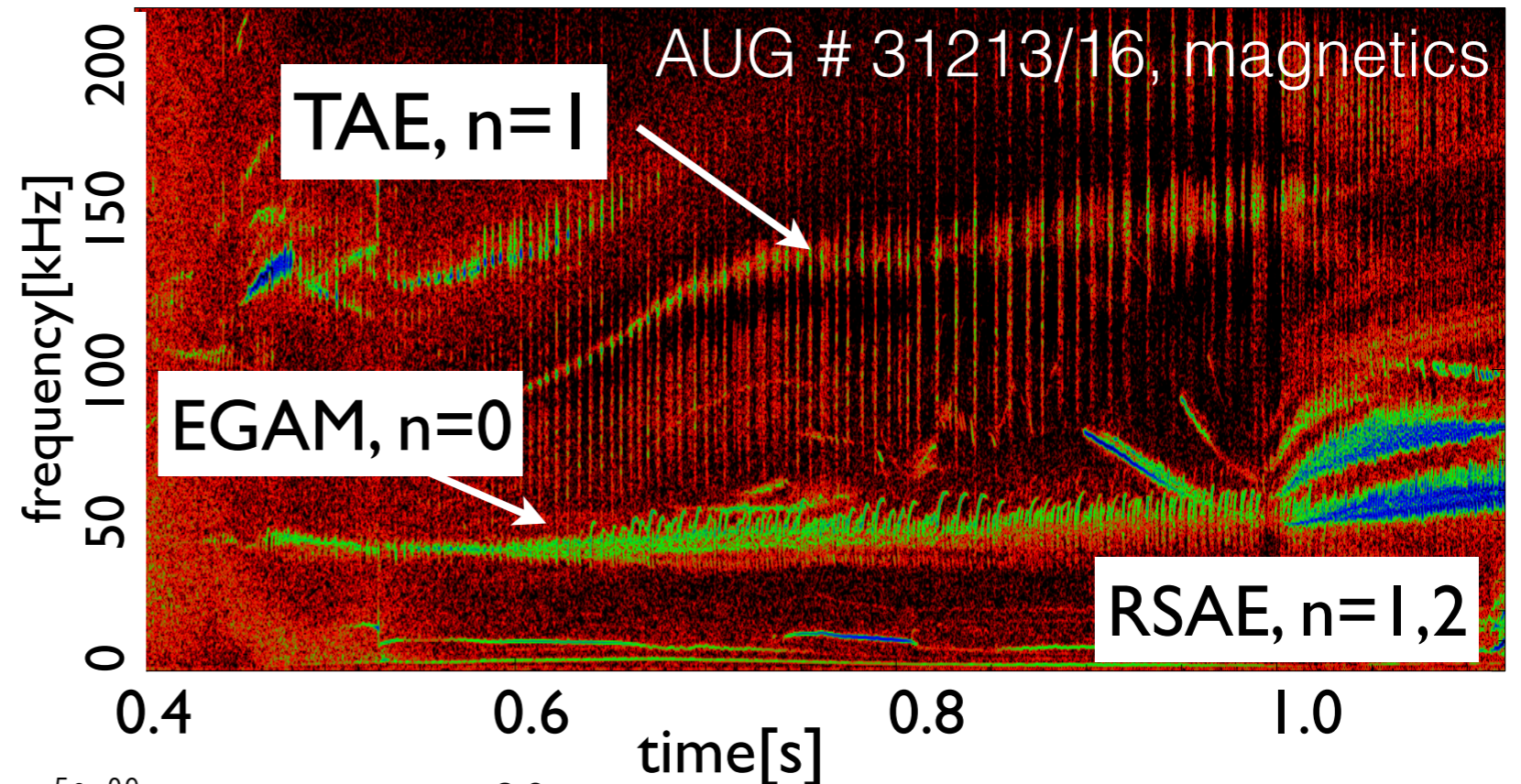
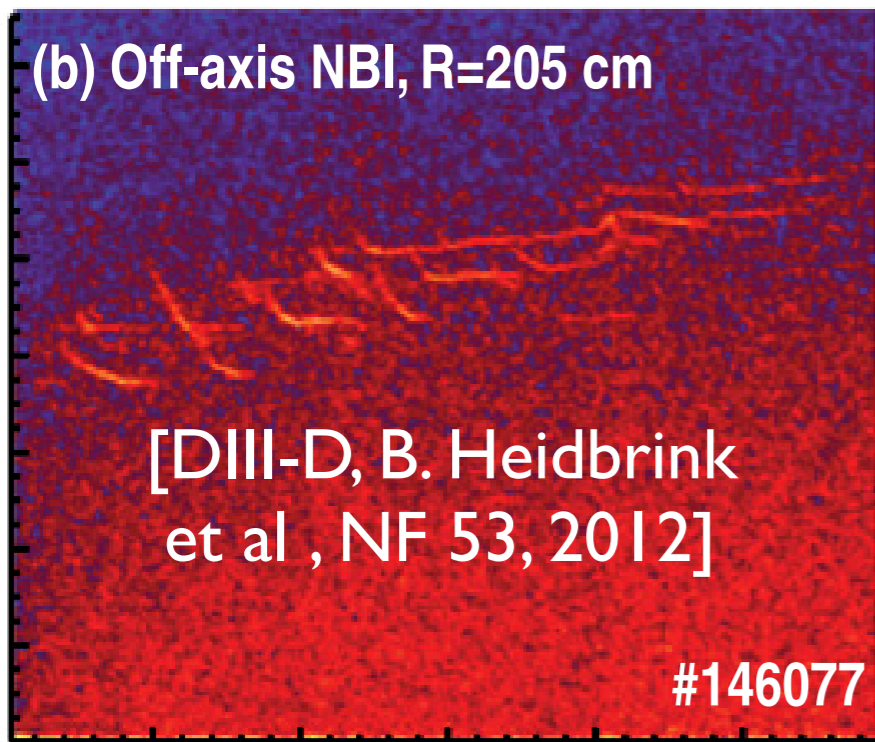


# Onset of strongly non-linear energetic-particle(EP)-driven modes in ASDEX Upgrade

Ph. Lauber with input from

I. Chavdarovski, A. Biancalani, M. Schneller, G. Fu,  
A. Bierwage, H. Wang, F. Palermo, P. Poloskei, G. Papp, G. Pokol, M. Maraschek  
and ASDEX Upgrade team



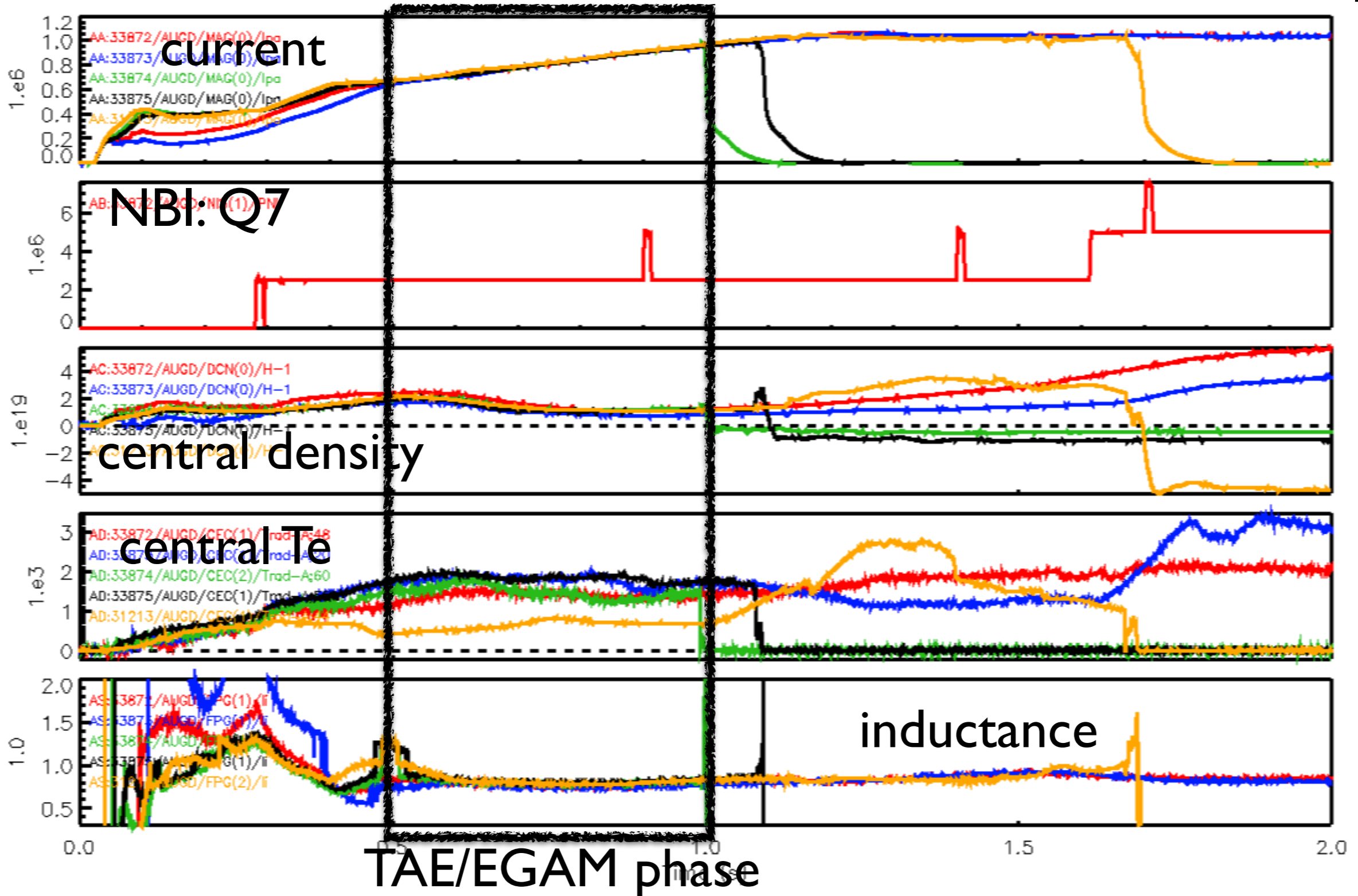
## the physics picture of this scenario:

- the accumulation of W in the core decreases the background Te, Ti and thus reduces the ion Landau damping of Alfvén eigenmodes (AEs); moves strong EP anisotropy in GAM frequency range
- often hollow Te profiles form
- large values of  $R_0 \nabla \beta_\alpha / \beta_{\text{back}}$  can arise, off-axis peaked EP distribution function forms; AEs propagating in both ion and electron diamagnetic direction; anisotropy in pitch angle drives EGAMs
- central ECRH can counteract this accumulation; the increased temperatures (strong EP anisotropy is ‘detuned’; increased Landau damping) bring the system below excitation threshold → threshold typically  $T_i \lesssim 1.8 \text{keV}$  for  $q \geq 2$
- $E_{\text{max}}/T_{i,\text{th}} \sim 90$  is comparable to burning plasma parameters (ITER/DEMO: 3.5 MeV/30 keV)
- opens possibility to study experimentally the interaction between Alfvénic modes, EGAMs i.e. zonal structures and background turbulence: due to the EGAM excitation a direct channel from EPs to n=0 modes can be investigated

strongly non-linear EP dynamics at AUG for sub-Alfvénic neutral beam injection raises the following questions:

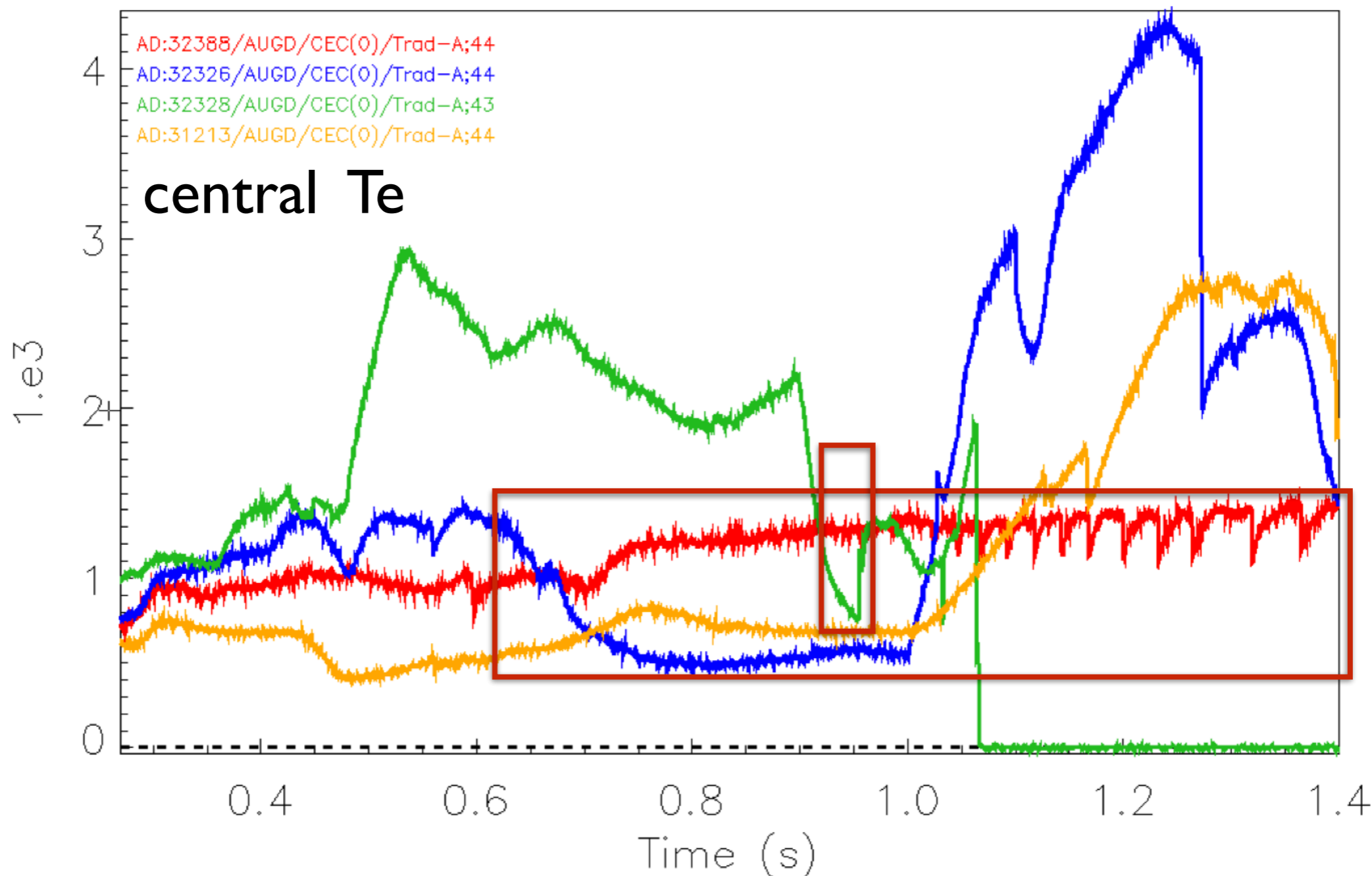
- experimental conditions?
- study non-linear evolution of various ES and EM modes
- study interaction between different modes (TAEs/RSAEs-EGAMs)
- study interaction of modes with turbulence [Zarzoso/Girardo 2015, Sasaki 2017; Duarte 2017]
- study scenarios that match projected DEMO parameters in  $\beta_{\text{fast}}/\beta_{\text{th}}$  and  $T_{\text{fast}}/T_{\text{th}}$
- why can system arrive at state well above marginal stability (critical gradient models would not allow for that state)?

obtain confidence in models and codes towards understanding the self-organisation of a burning plasma;  
low- $\beta$  turbulence-EGAM interaction allows to use electrostatic limit



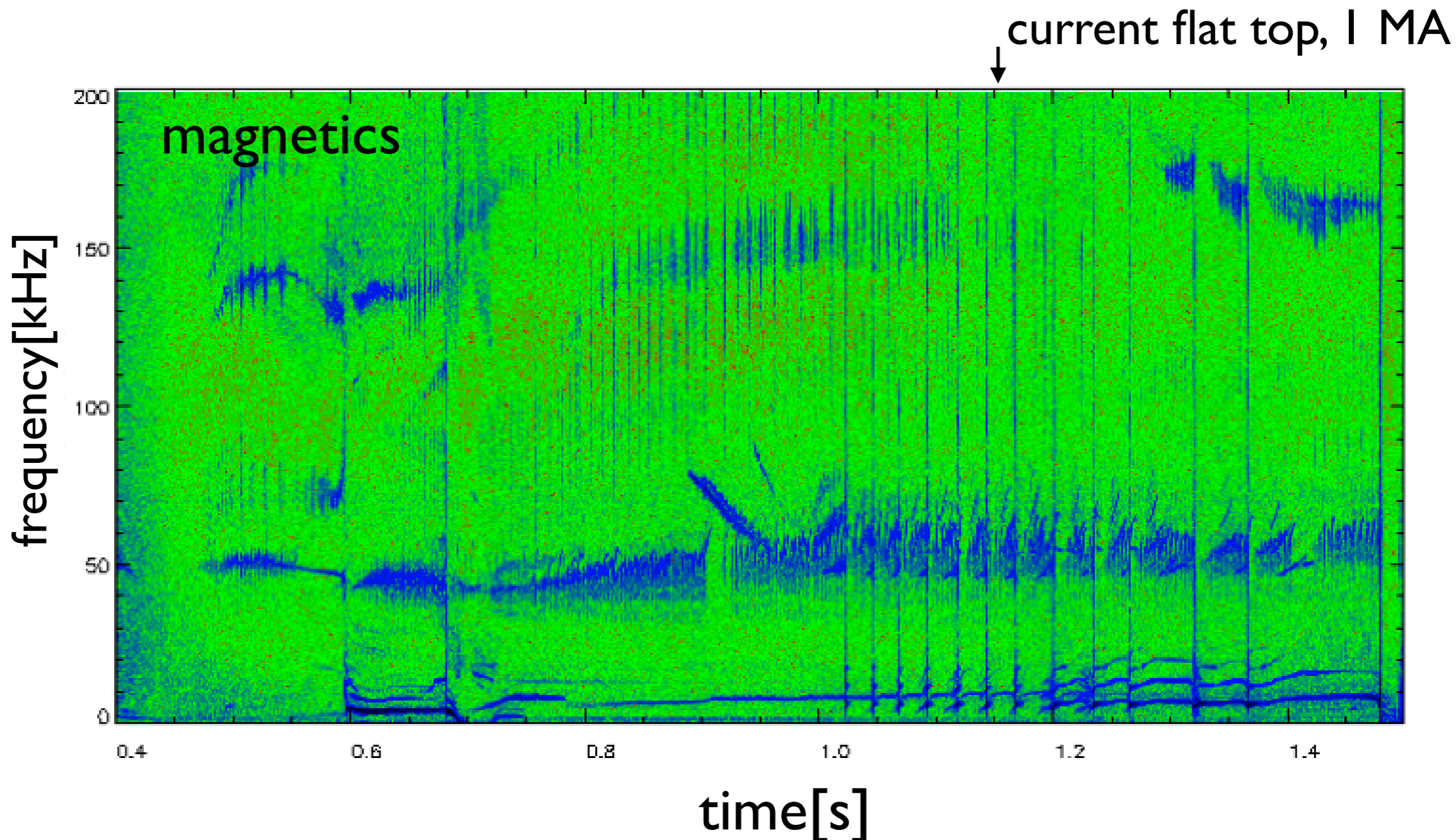
well reproducible scenario

onset conditions for EGAMs ( $T_i \approx 1.8\text{keV}; T_e < T_i \text{ } q \geq 2$ )  
confirmed by **new** experiments

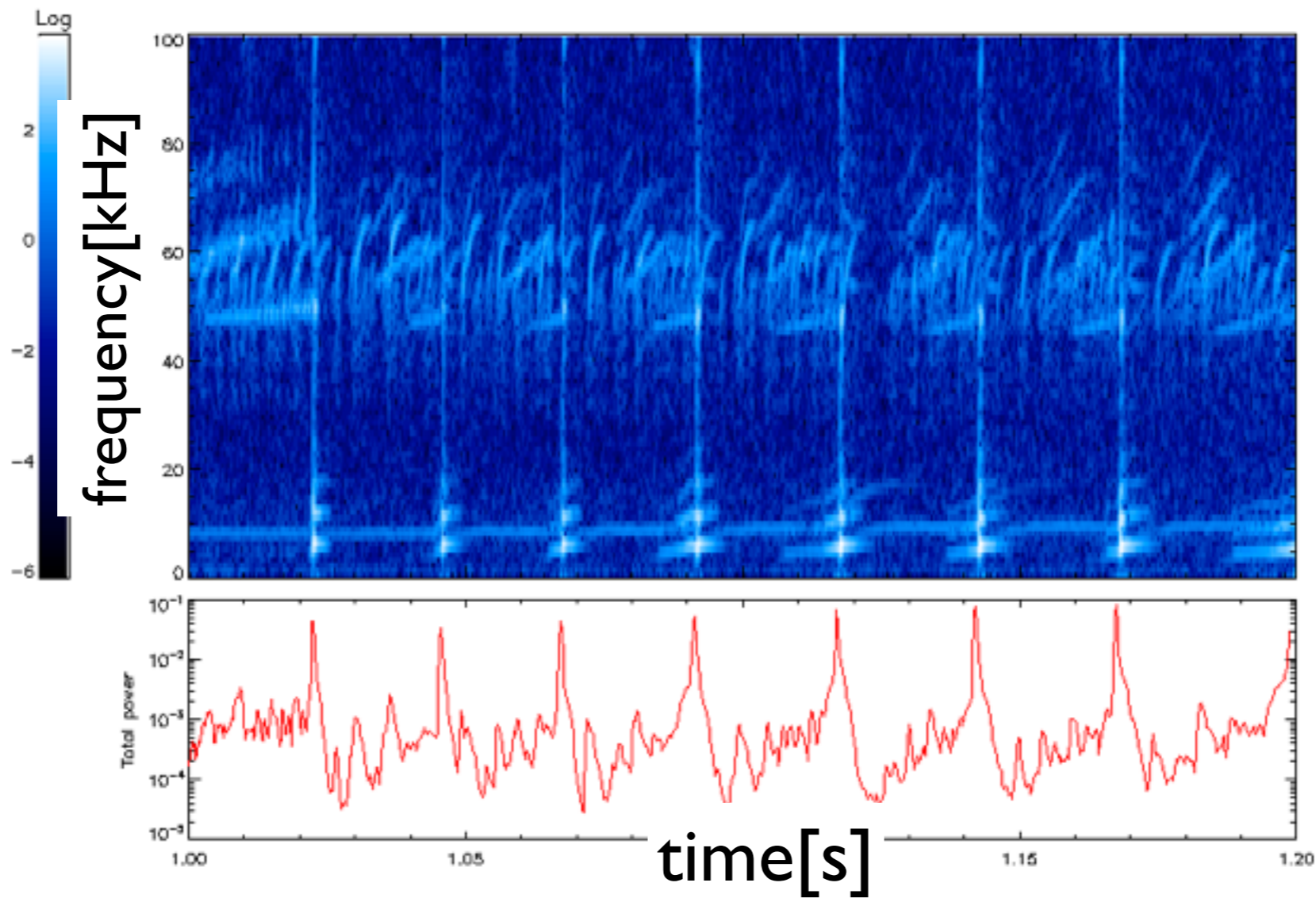


longer, more stable phases with EGAMs in new experiments

- slightly higher density: more stable transition through  $q=2/q_{\text{edge}}=4$  region
- optimised beam blips for measuring  $T_i$



# regular sawtooth like crashes at $q=2$ surface

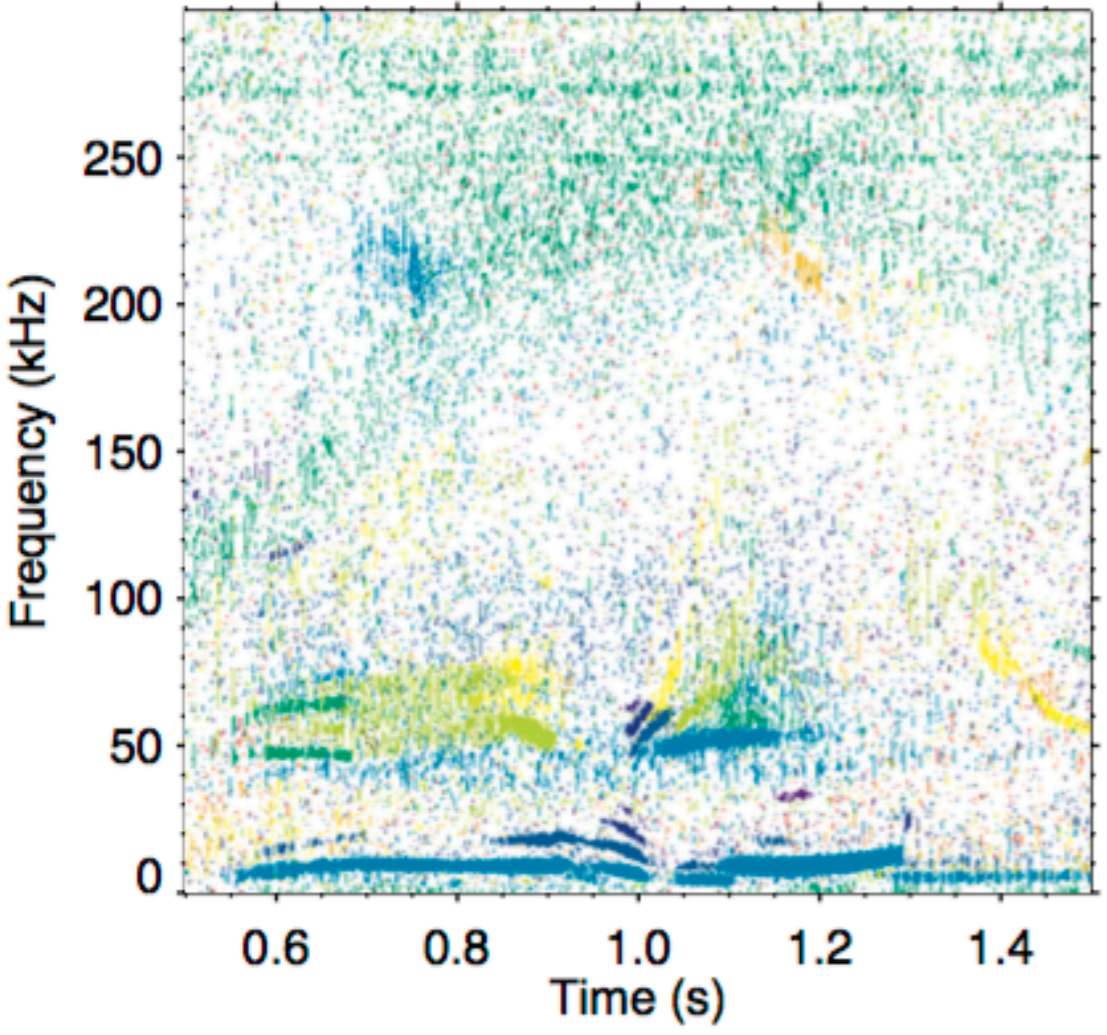


- $q=2$  sawtooth crashes like in 2001-05 JET/JT60U discharges (current holes) - is this how advanced scenarios JT-60SA will look like? [A Bierwage, 2016/17]
- EGAMs persistent during these crashes
- surprisingly no variation of EGAM onset frequency - constant  $T_i$ !

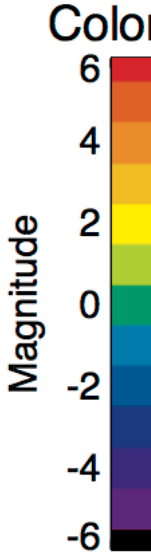
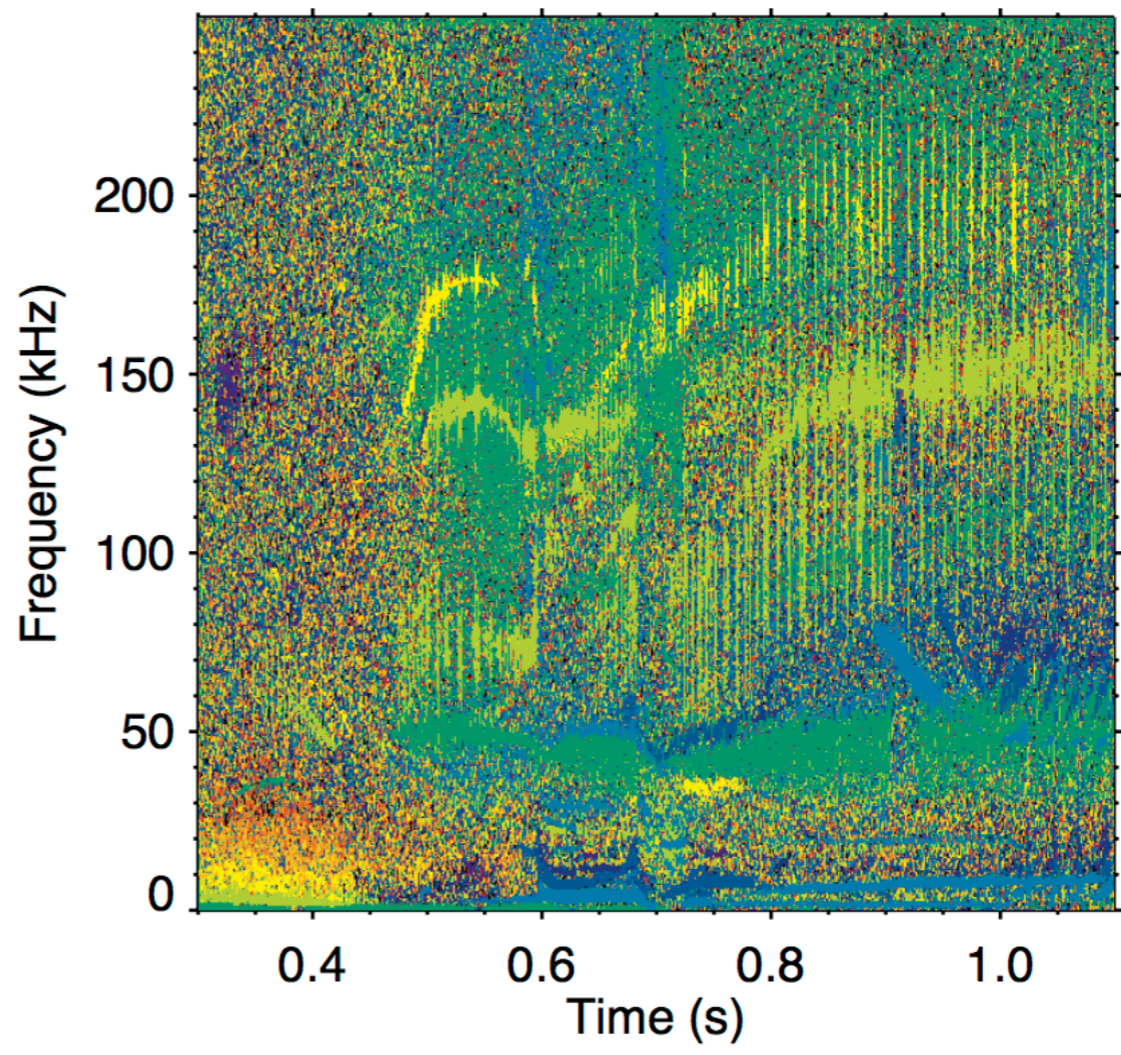


# instability threshold for EGAM observed no Te inversion

Toroidal mode numbers of AUGD 33872



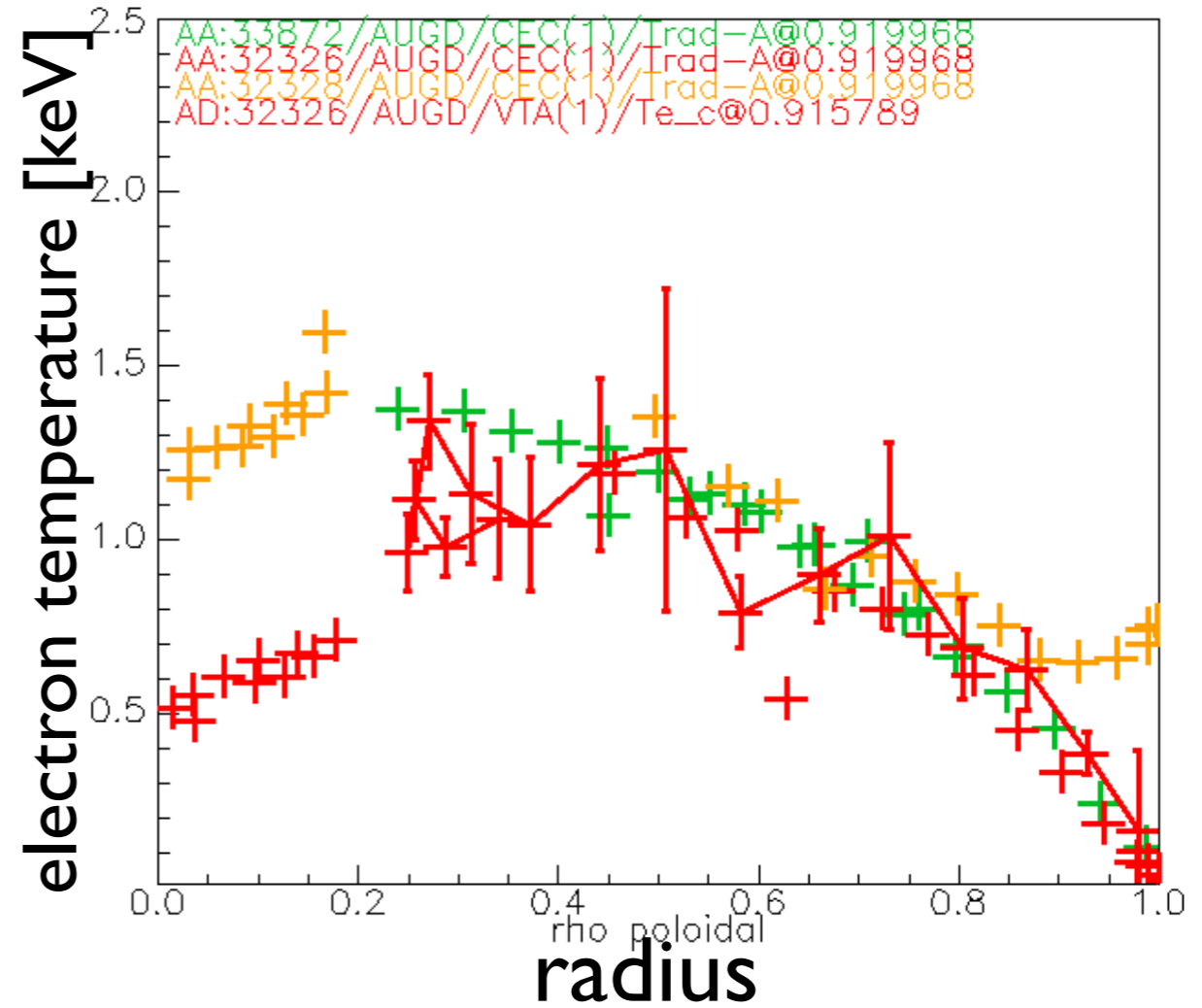
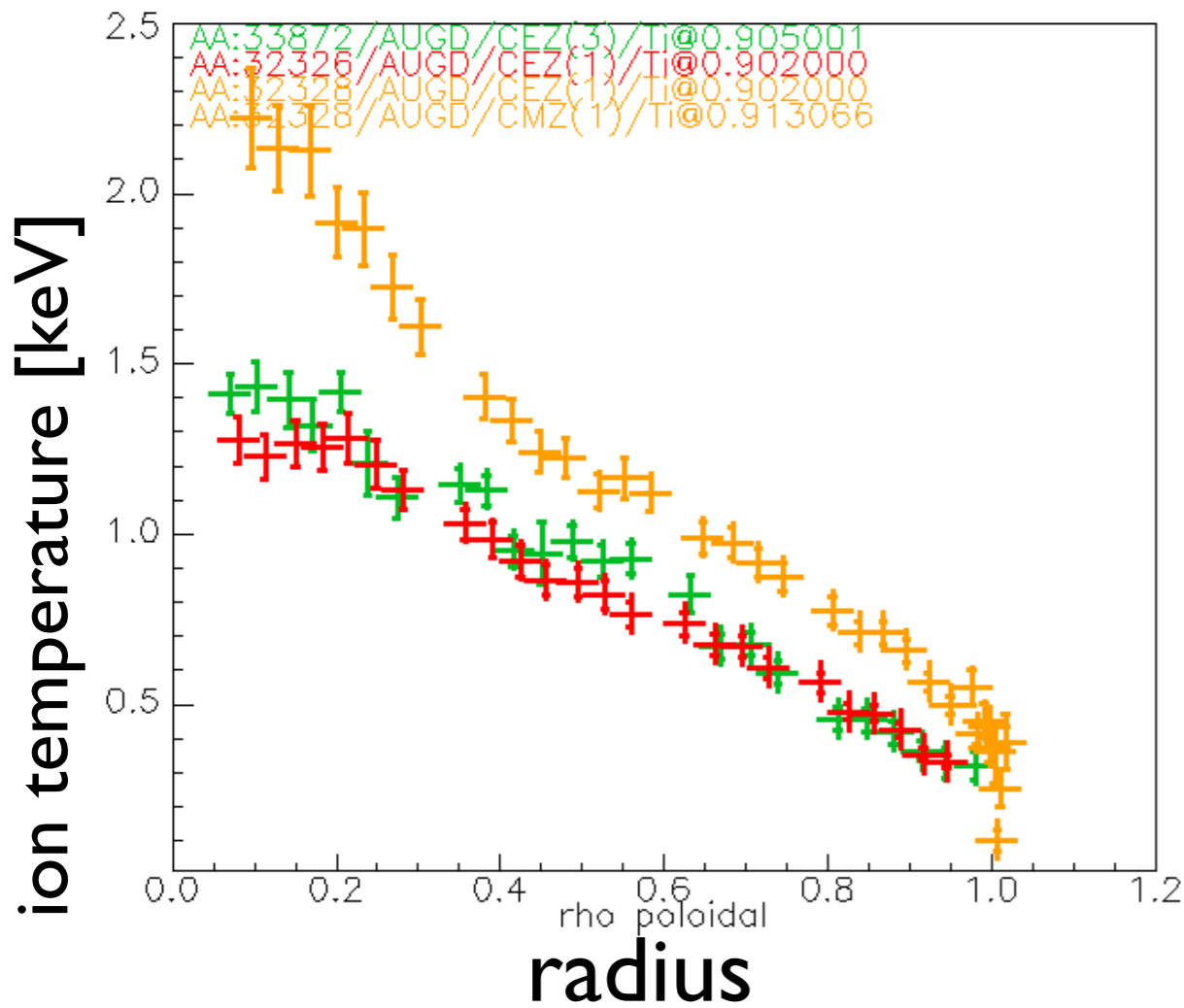
Toroidal mode numbers of AUGD 32388

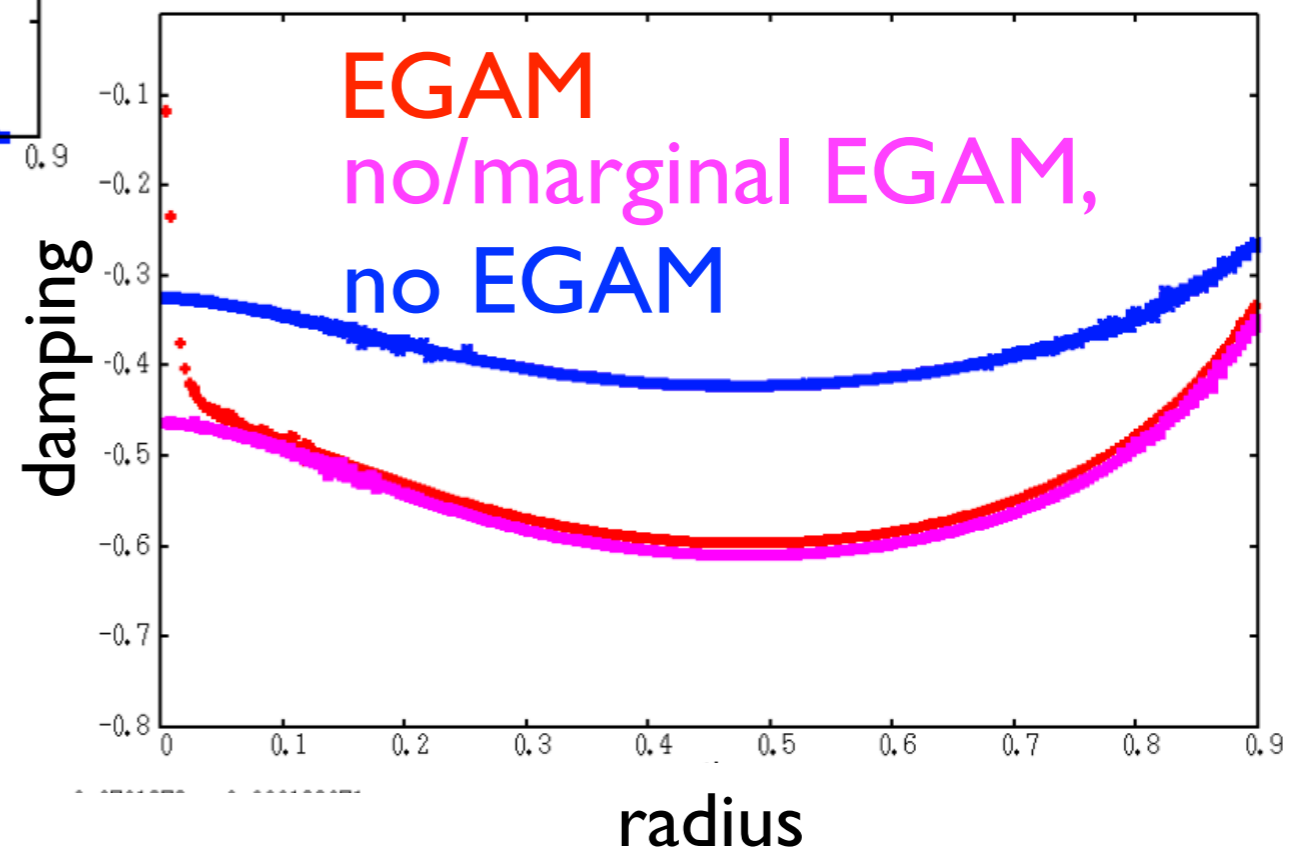
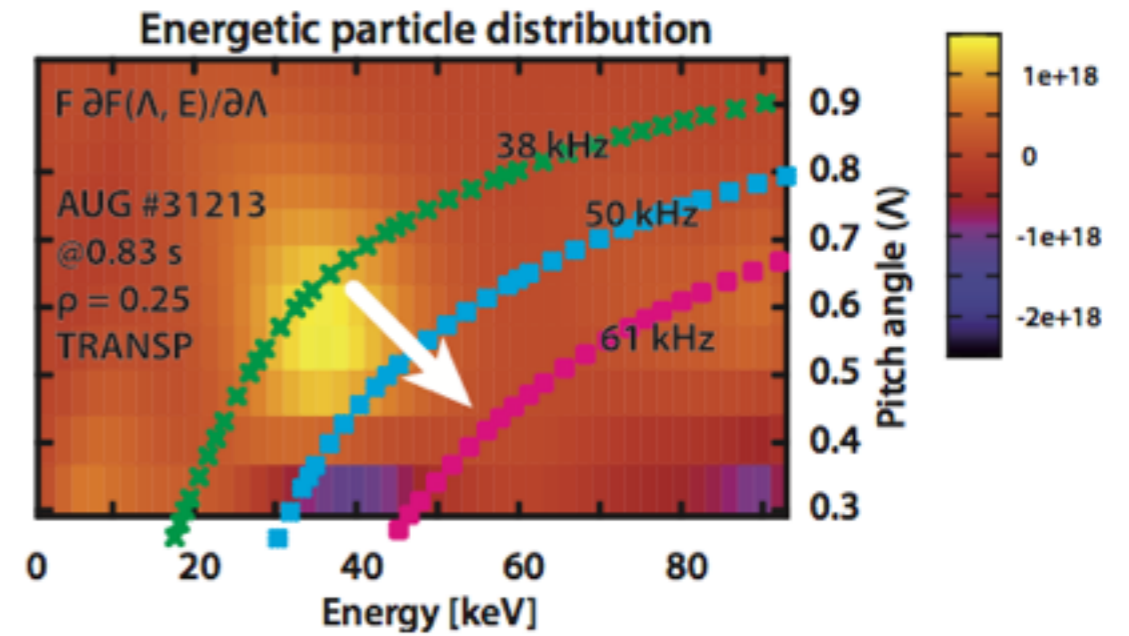
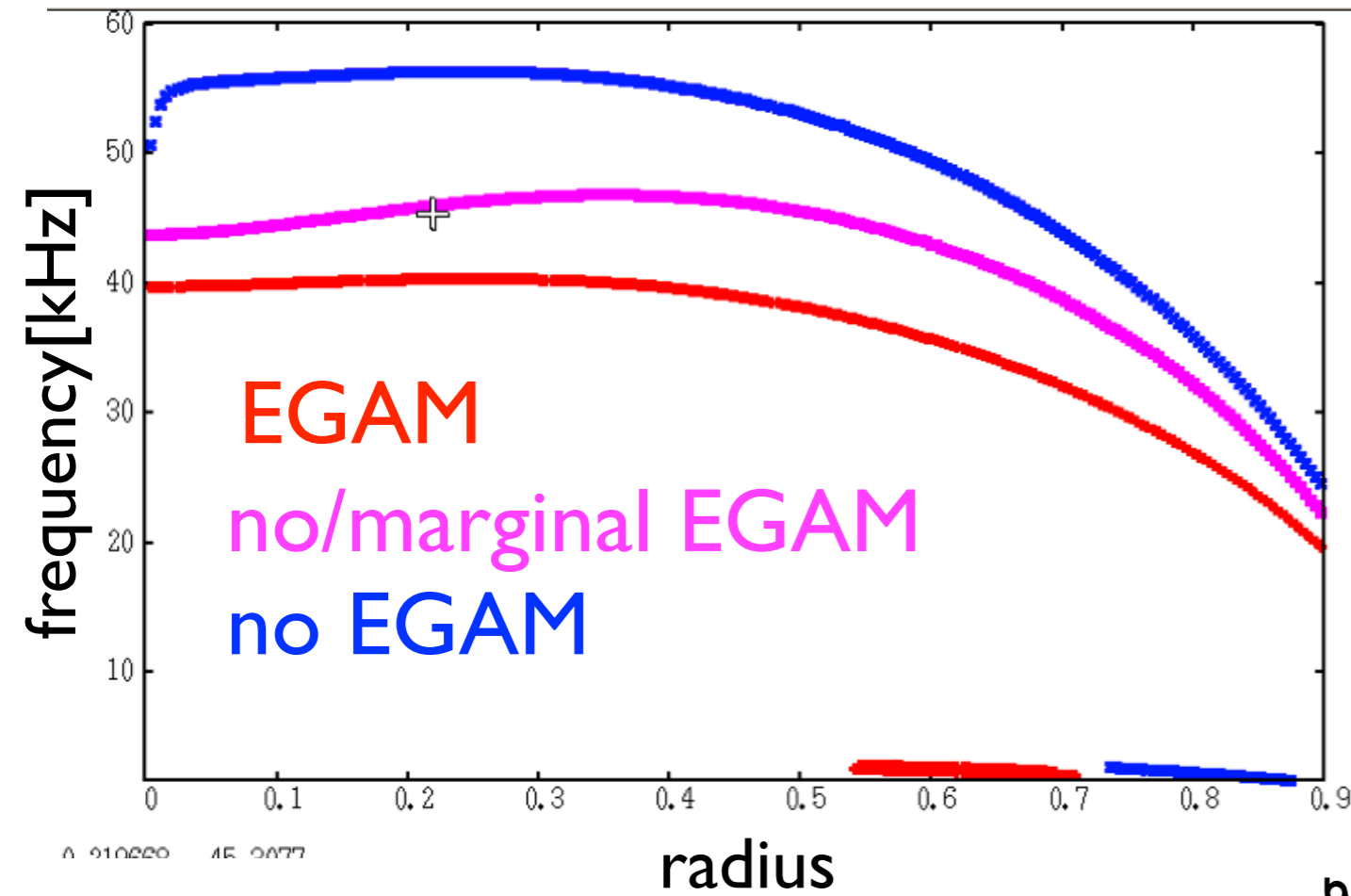


Time stamp: /afs/ipp  
version: 1.8.0  
shot: AUGD 32388  
window: Gauss  
winsize: 250  
0.00050000127s  
ires: 1000  
step: 333  
averages: 0  
filter: Rel. pos.  
mode steps: 1.000  
Coherence limit: 0.0  
Power limit: 0.0000  
Q limit: 100 %  
channel pairs: 15  
MHA-B31-14-MHA  
MHA-B31-14-MHA  
MHA-B31-14-MHA  
MHA-B31-14-MHA  
MHA-B31-14-MHA  
MHA-B31-03-MHA  
MHA-B31-03-MHA  
MHA-B31-03-MHA  
MHA-B31-03-MHA  
MHA-B31-01-MHA

q-profile evolution similar: timing and slope of RSAEs similar

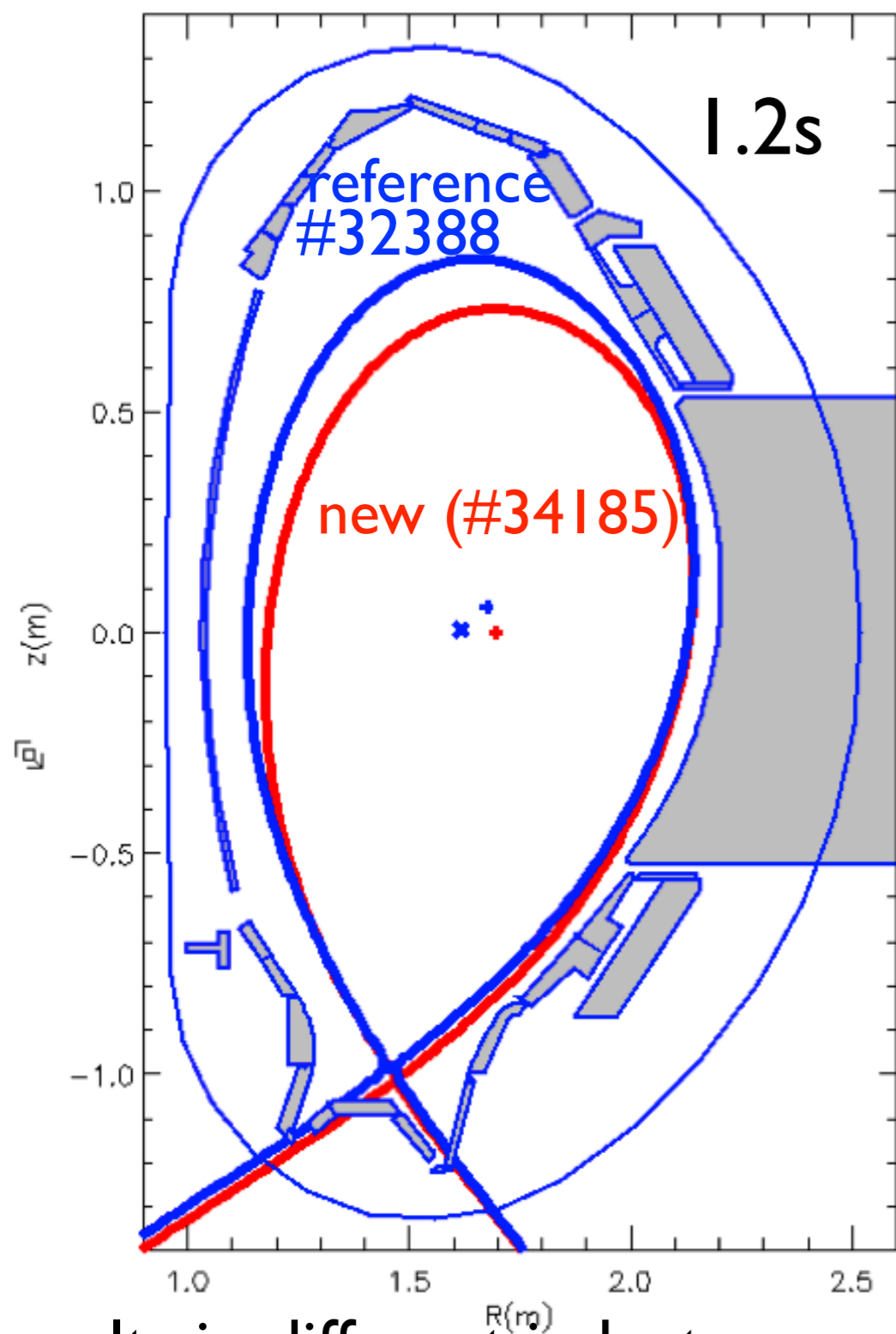
discharge with EGAM  
 discharge without EGAM  
 discharge at marginal stability of EGAM



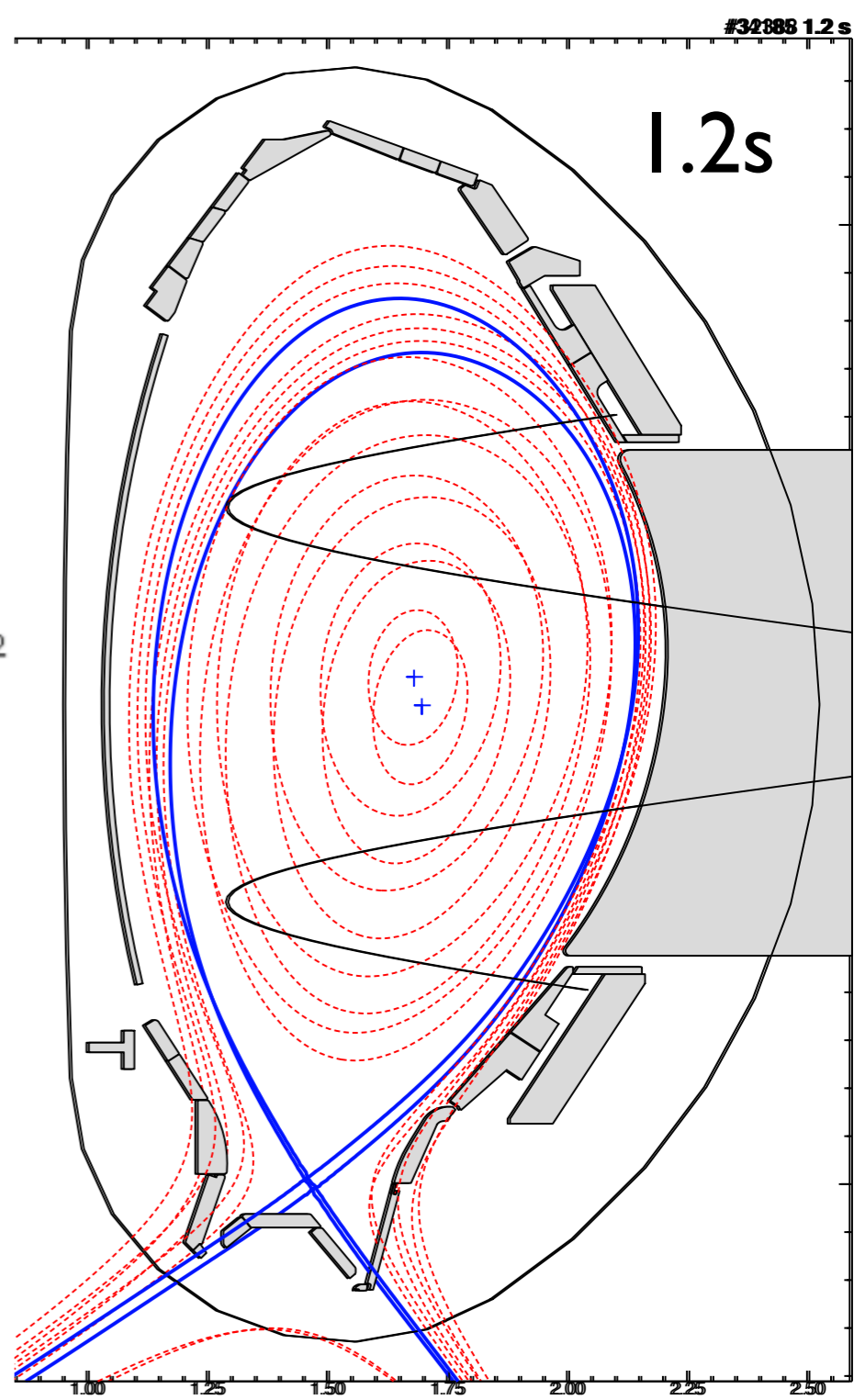


- both Ti and Te important for mode stability;
- strongest anisotropy has to match GAM continuum
- other effects important? propagation?

# modification of plasma position and shape after $t > 0.8s$ : mainly different NB deposition position



AUG Flux: $\rho_{pol}$	AUG Flux: $\psi_{pol}$
AUGD/EQI(1)	AUGD/EQI(1)
AUGD/EQI(1)	Shot: 34185
Shot: 32388	Time: 1.200
Time: 1.200	
From GQI	From GQI
$I_p$ : 1.02MA	$I_p$ : 1.01MA
$\beta_p$ : 0.21	$\beta_p$ : 0.23
$\zeta_1$ : 0.91	$\zeta_1$ : 0.84
ma: 1.677 : 0.05	ma: 1.698 : -0.002
cc: 1.619 : 0.007	cc: 1.640 : -0.063
$\delta_x$ : -0.022	$\delta_x$ : -0.082
$\delta_y$ : 0.361	$\delta_y$ : 0.389
$\kappa$ : 1.742	$\kappa$ : 1.728
$a_{hor}$ : 0.497m	$a_{hor}$ : 0.478m
$q_{95}$ : -3.88	$q_{95}$ : -3.52
$R_{aus}$ : 2.144m	$R_{aus}$ : 2.142m
vol : 13.45m <sup>3</sup>	vol : 12.44m <sup>3</sup>
$\Delta_b$ : 0.058m	$\Delta_b$ : 0.058m
$z_{gr}$ : -1.116m	$z_{gr}$ : -1.150m
$z_{ga}$ : -1.346m	$z_{ga}$ : -0.801m

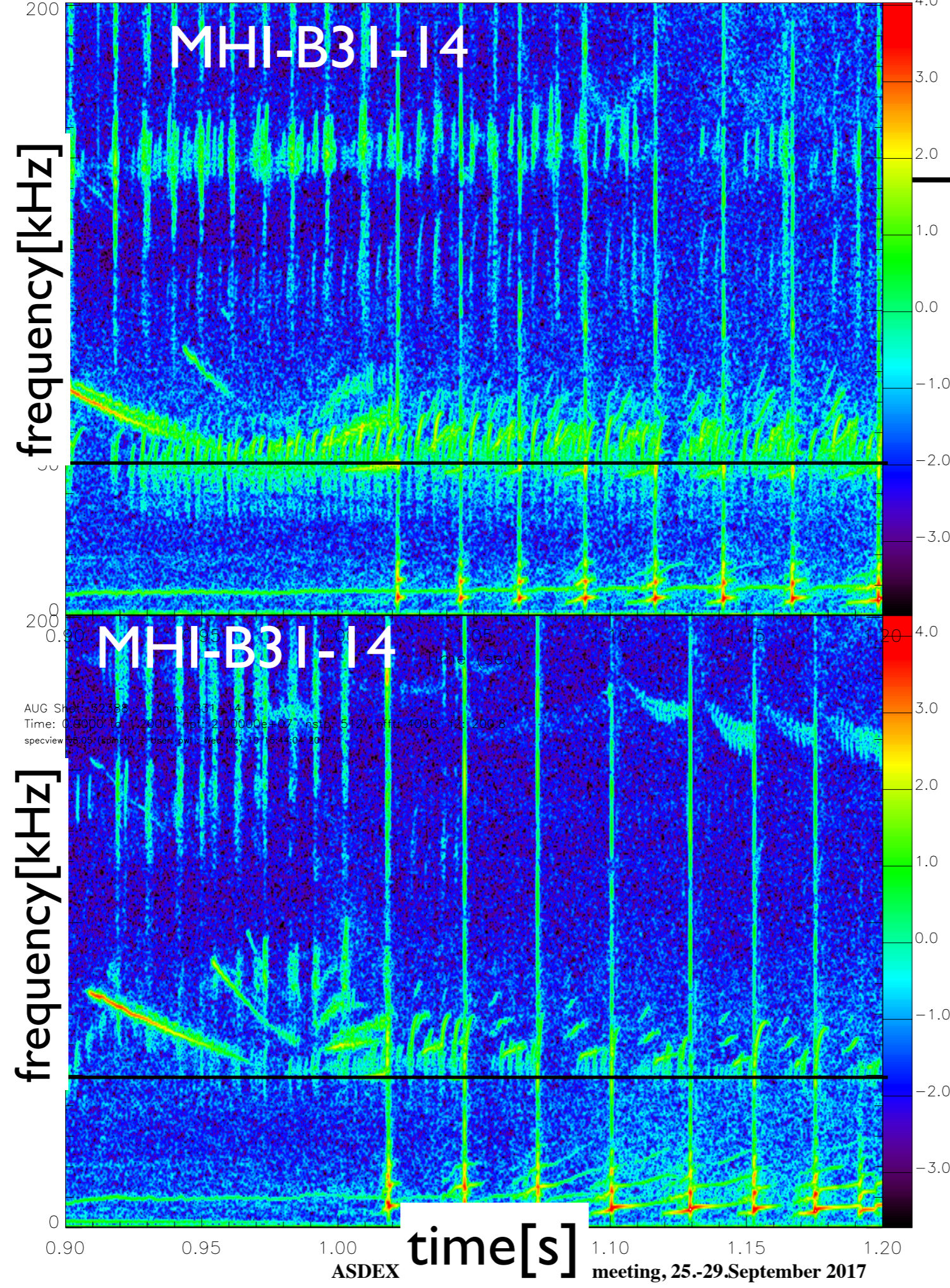


results in different inductance, q-profile, elongation [thanks to Th Pütterich]

scenario developed further (II)

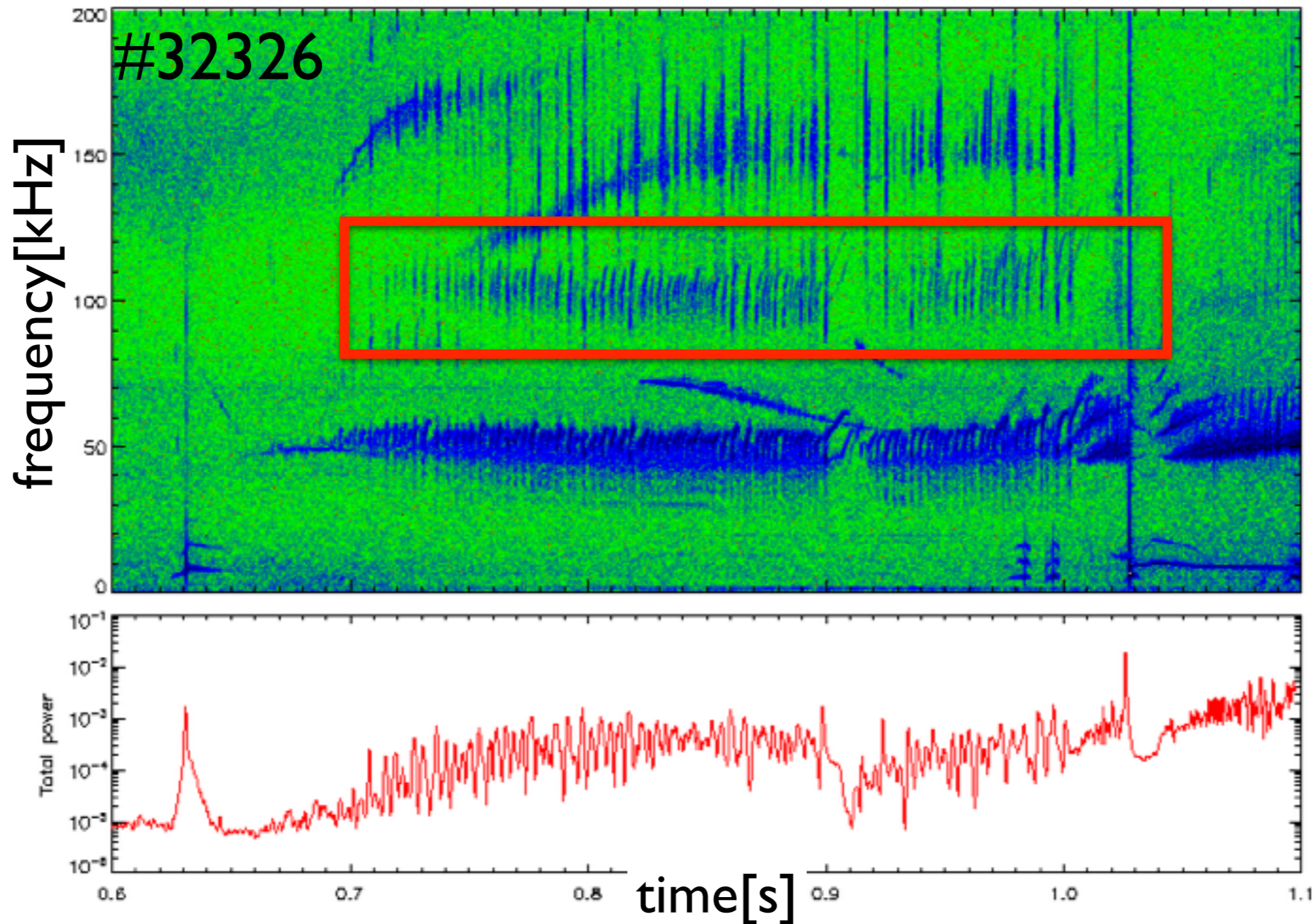
reference (#32388)

new shape (#34185)



- different dynamics for:
- TAEs
  - EGAMs
  - TAE/EGAM coupling
  - $q=2$  crashes

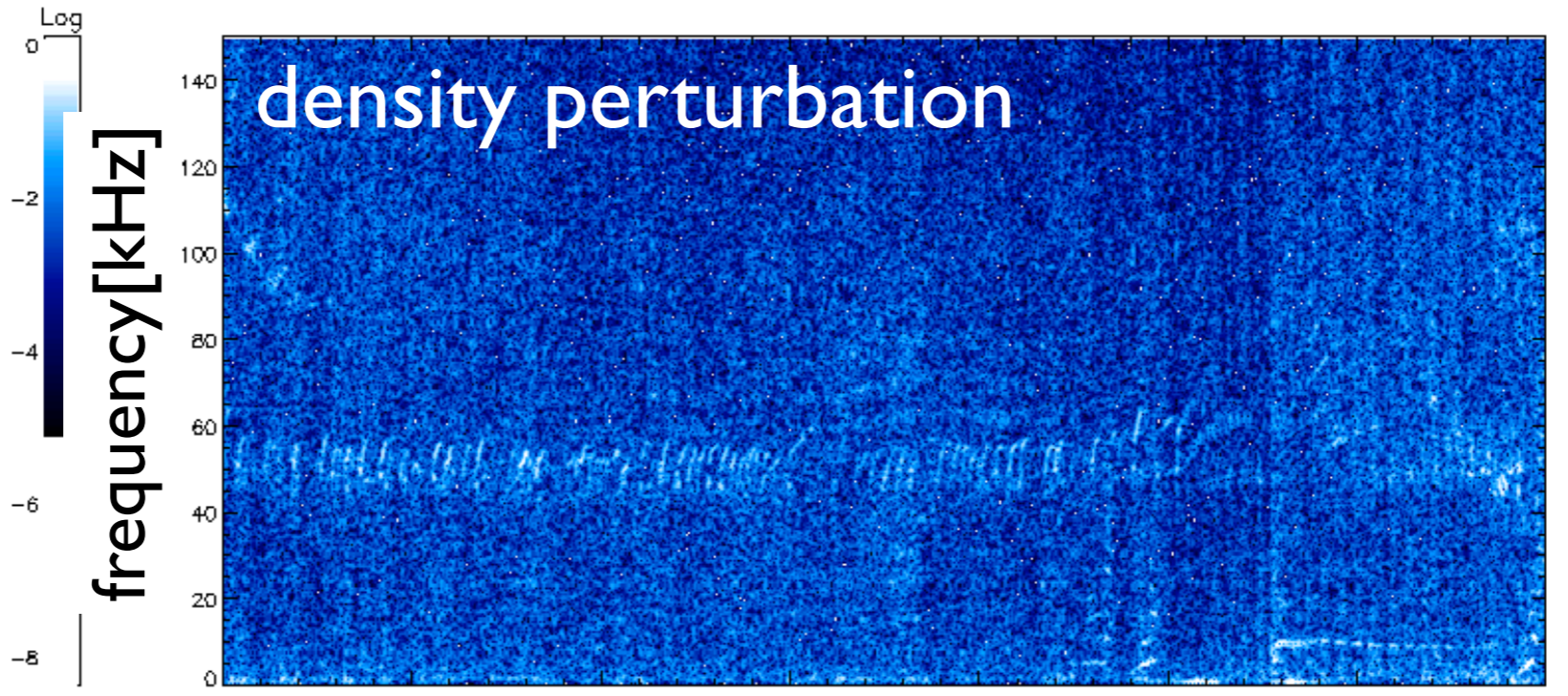
almost no difference in profiles; details of NB distribution function seem to be responsible



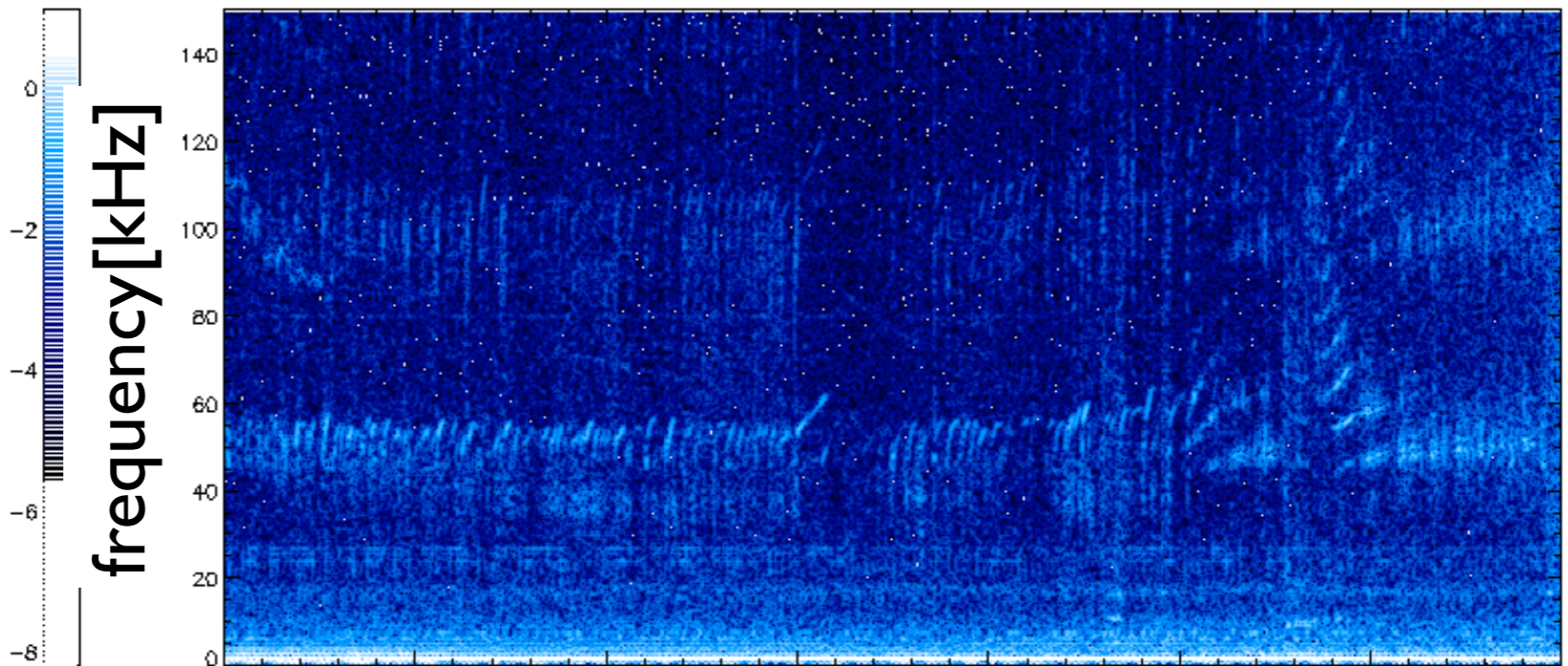
2nd order EGAM excitation: signature of density perturbation

DIII-D, Fu [2011]: 2nd order outboard midplane density perturbation is comparable to first-order perturbation

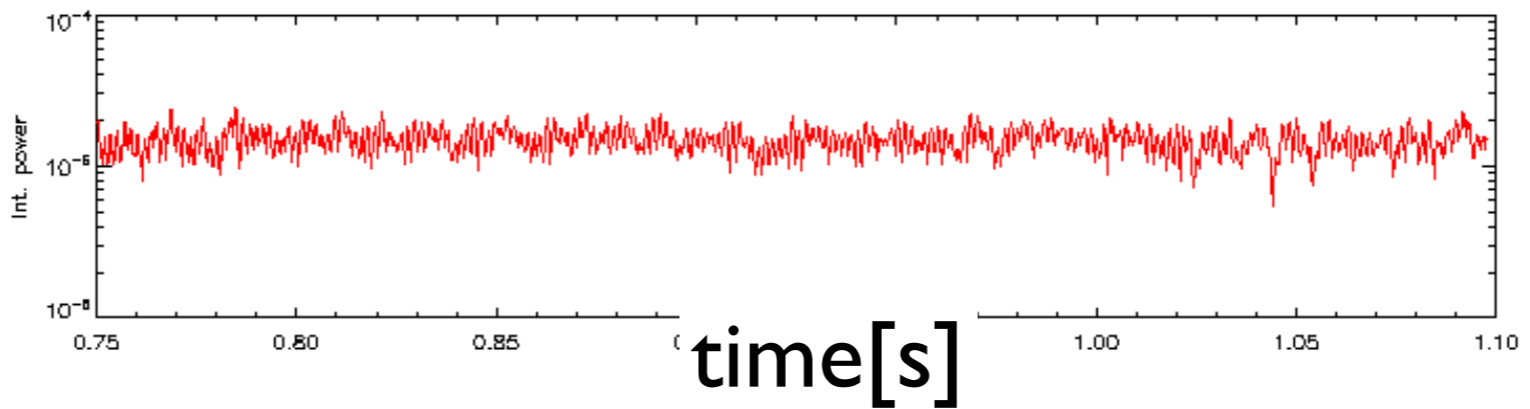
at  
AUG:  
first order  
EGAM  
harmonics  
dominates,  
2nd order  
perturbation  
more visible  
on high field  
side



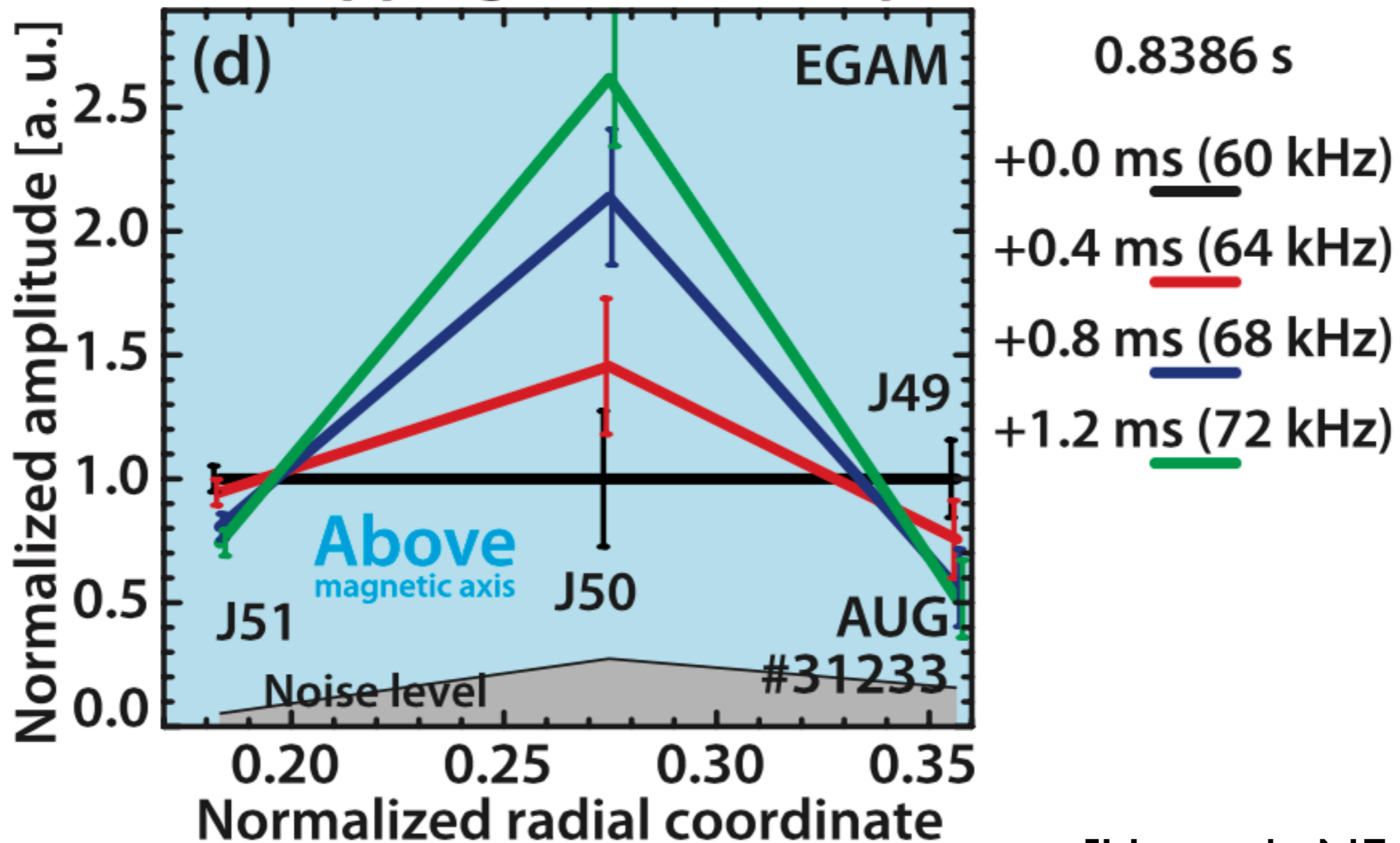
reflectometry:  
low field side



reflectometry  
high field side



### Radial mapping of mode amplitude



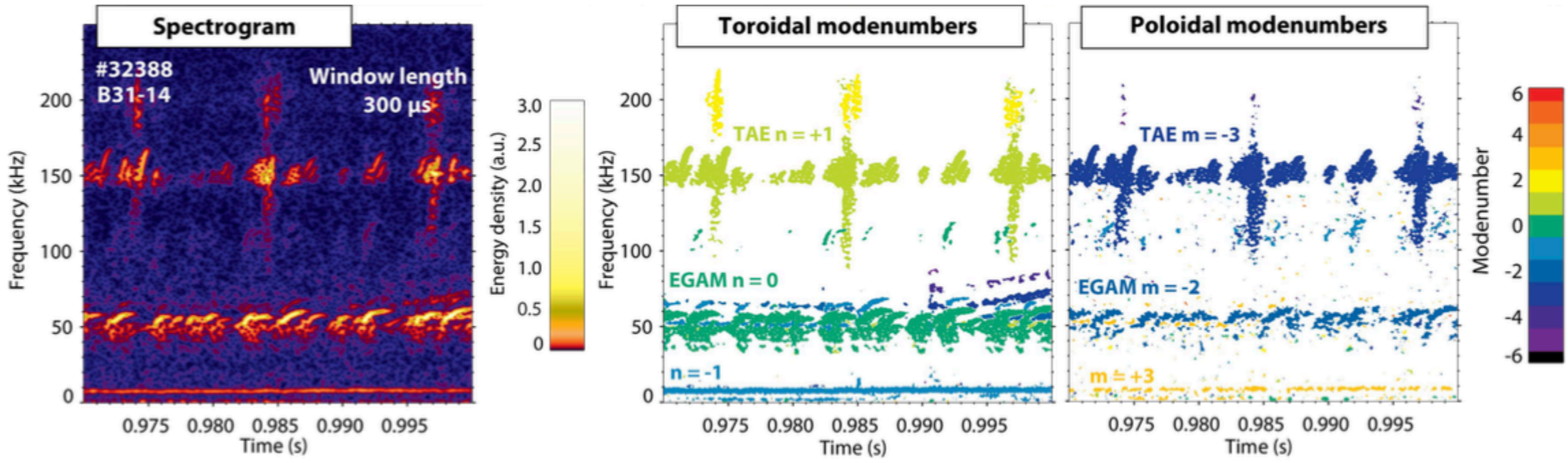
[Horvath, NF 2016]

radial position agrees with reflectometry data, interferometer



- Chirping EGAMs at ~50 kHz with (-2,0)  
(propagating in electron diamagnetic direction)
- Chirping/bursting TAEs at ~150 kHz with (-3,+1)

**AUG #32388**

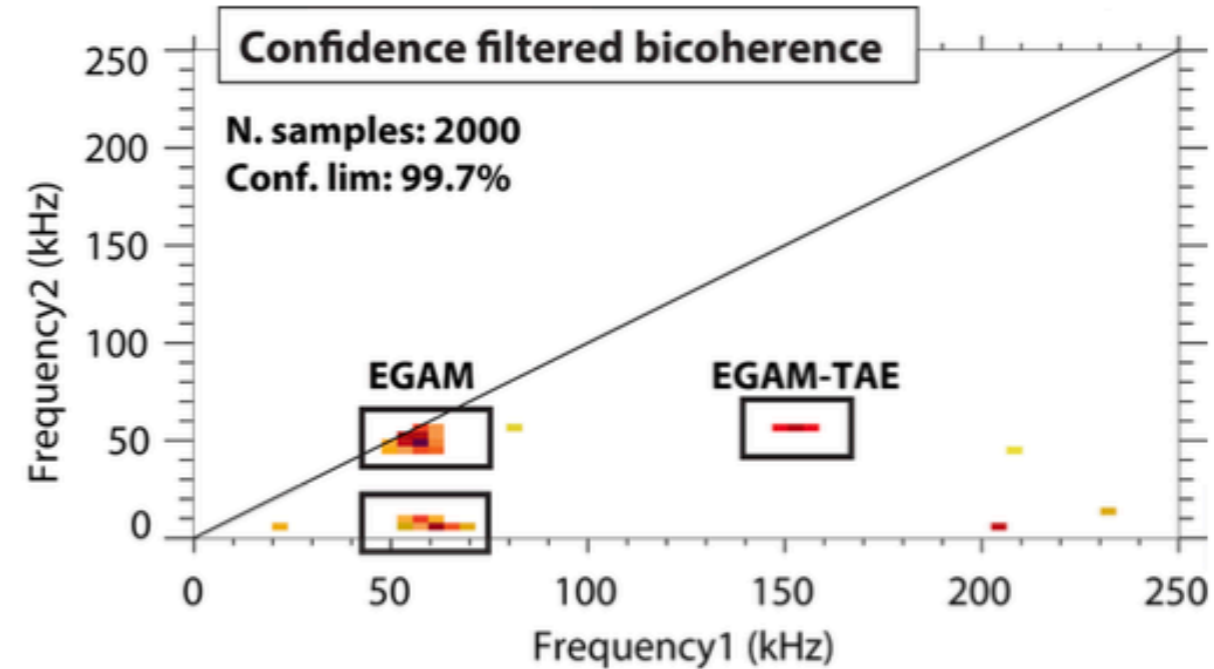
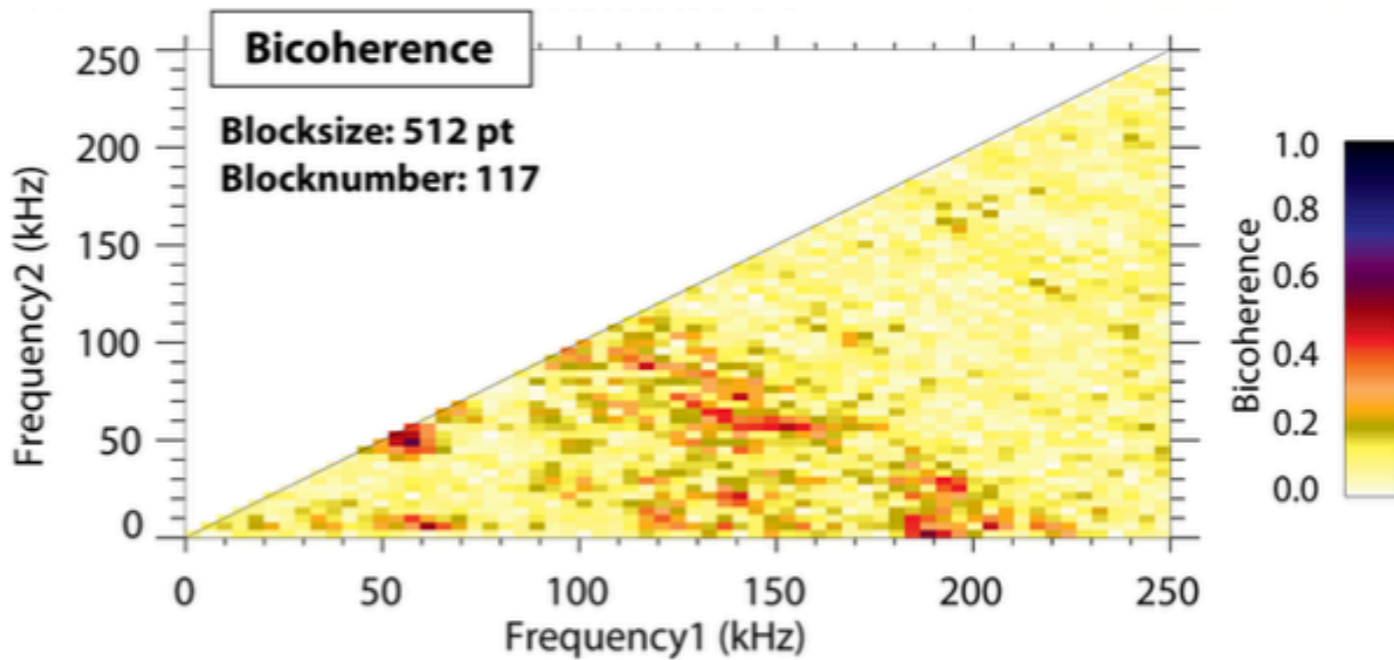


signals with rapid chirping (amplitudes, frequency) may cause 'spurious' bicoherence

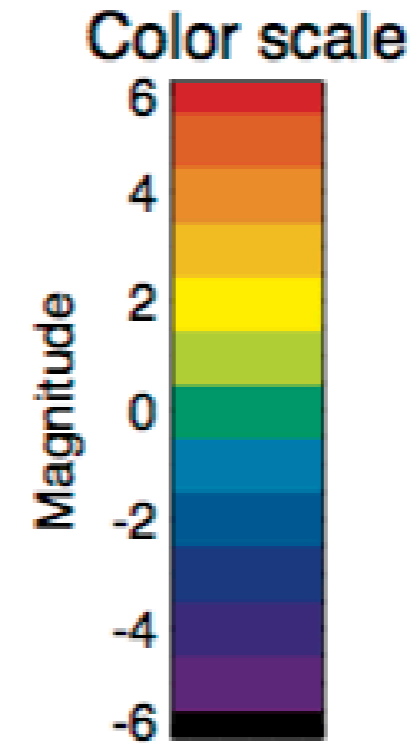
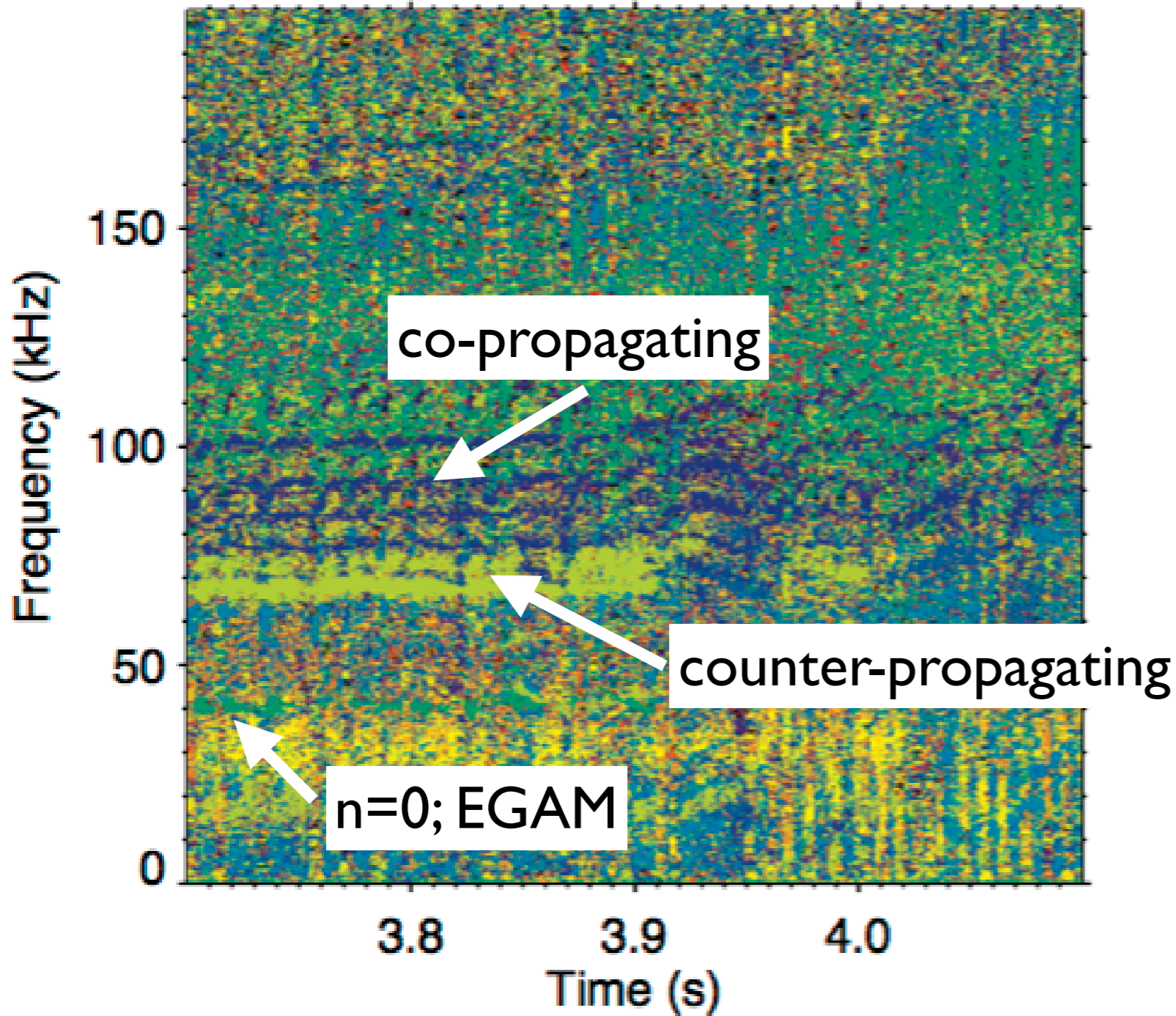
# phase randomized bicoherence probability density function calculation

- High bicoherence around at (55, 55) kHz indicates **strongly nonlinear EGAMs**. (see spectrogram at ~110 kHz)
- **Without filtering interaction with TAEs is not clear**

- Filtering shows high, significant bicoherence around (155, 55) kHz
- **Indicates the nonlinear interaction between EGAMs and TAEs**



### Toroidal mode numbers of AUGD 34200



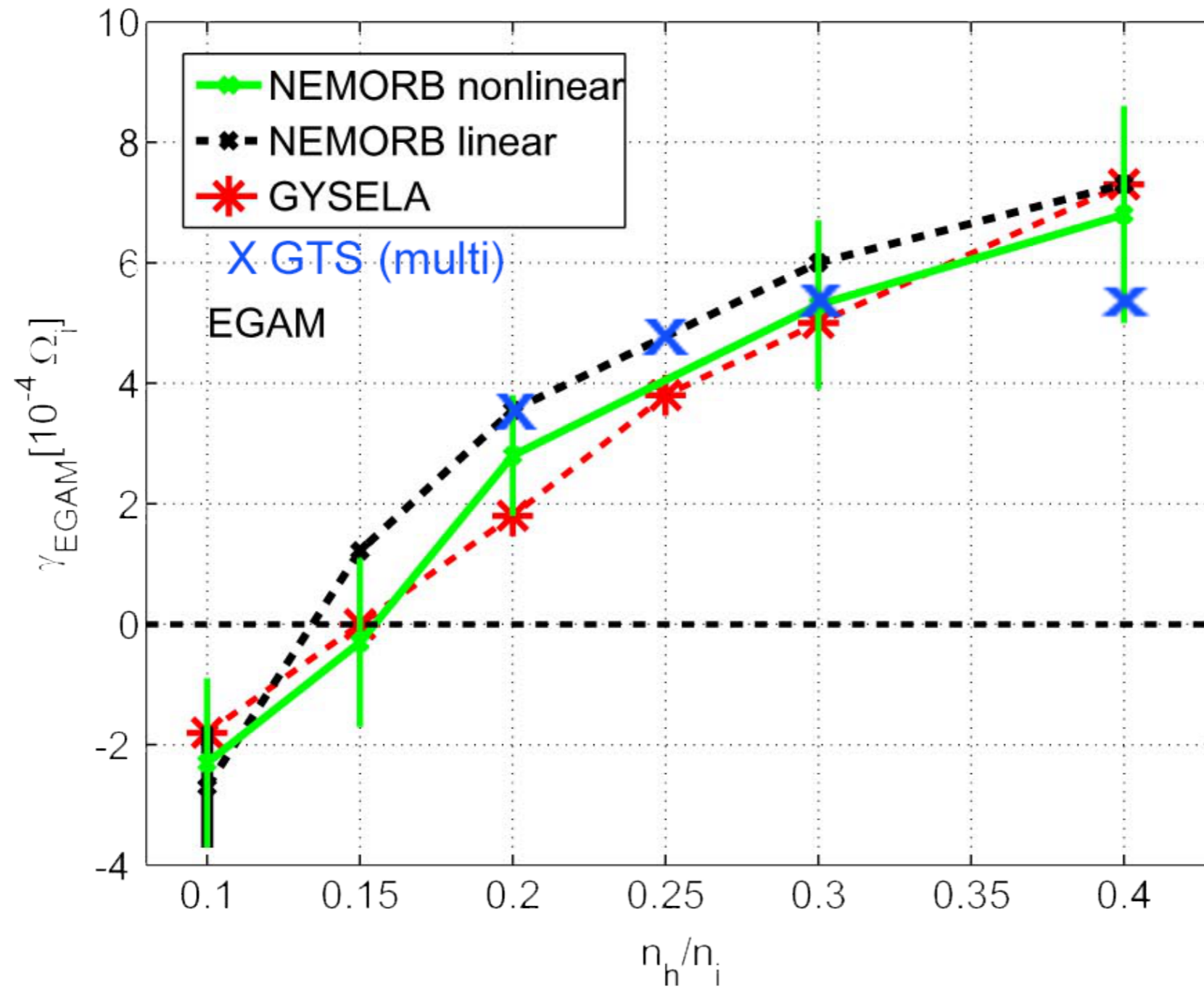
Time stamp: /afs/ipp-garching.mpg.de/hon  
version: 1.7.1  
shot: AUGD 34200  
window: Gauss  
wsize: 1000  
0.00250000042s  
freq: 4000  
step: 40  
averages: 0  
filter: Rel\_pos  
mode steps: 1  
Coherence limit: 0.00000 %  
Power limit: 0.00000 %  
Q limit: 100 %  
Channel pair: 21  
Mn: 831-40-Mn: 831-14  
Mn: 831-40-Mn: 831-03  
Mn: 831-40-Mn: 831-01  
Mn: 831-40-Mn: 831-02  
Mn: 831-40-Mn: 831-12  
Mn: 831-14-Mn: 831-03  
Mn: 831-14-Mn: 831-01  
Mn: 831-14-Mn: 831-02  
Mn: 831-14-Mn: 831-12

## AUG data inspired wide-spread theory efforts:

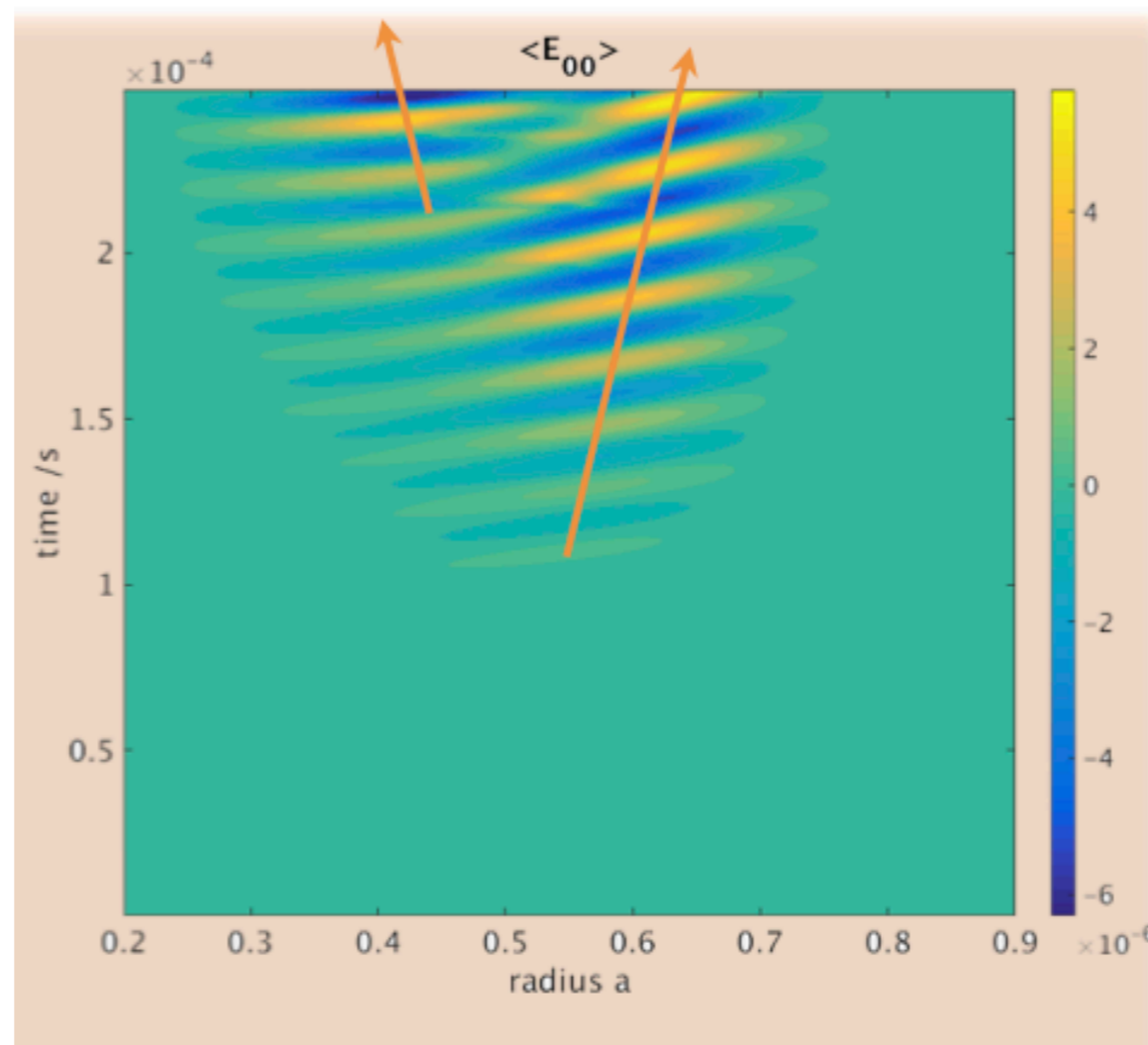
- ENR NLED (Zonca);
  - ENR NAT (Lauber);
  - MPPC: M. Schneller, (GTS), I. Chavdarovski
  - QST, Japan: H. Wang (MEGA), A Bierwage (LIGKA)
- } Biancalani:ORB5; X. Wang: XHMGC;  
A. Mishchenko: Euterpe, Lauber: LIGKA
- linear drive
  - radial propagation
  - non-linear interaction: wave-wave
  - non-linear interaction: wave-particle

# linear EGAM physics: codes agree rather well

Growth rate vs fast-ion concentration, with adiabatic elec.



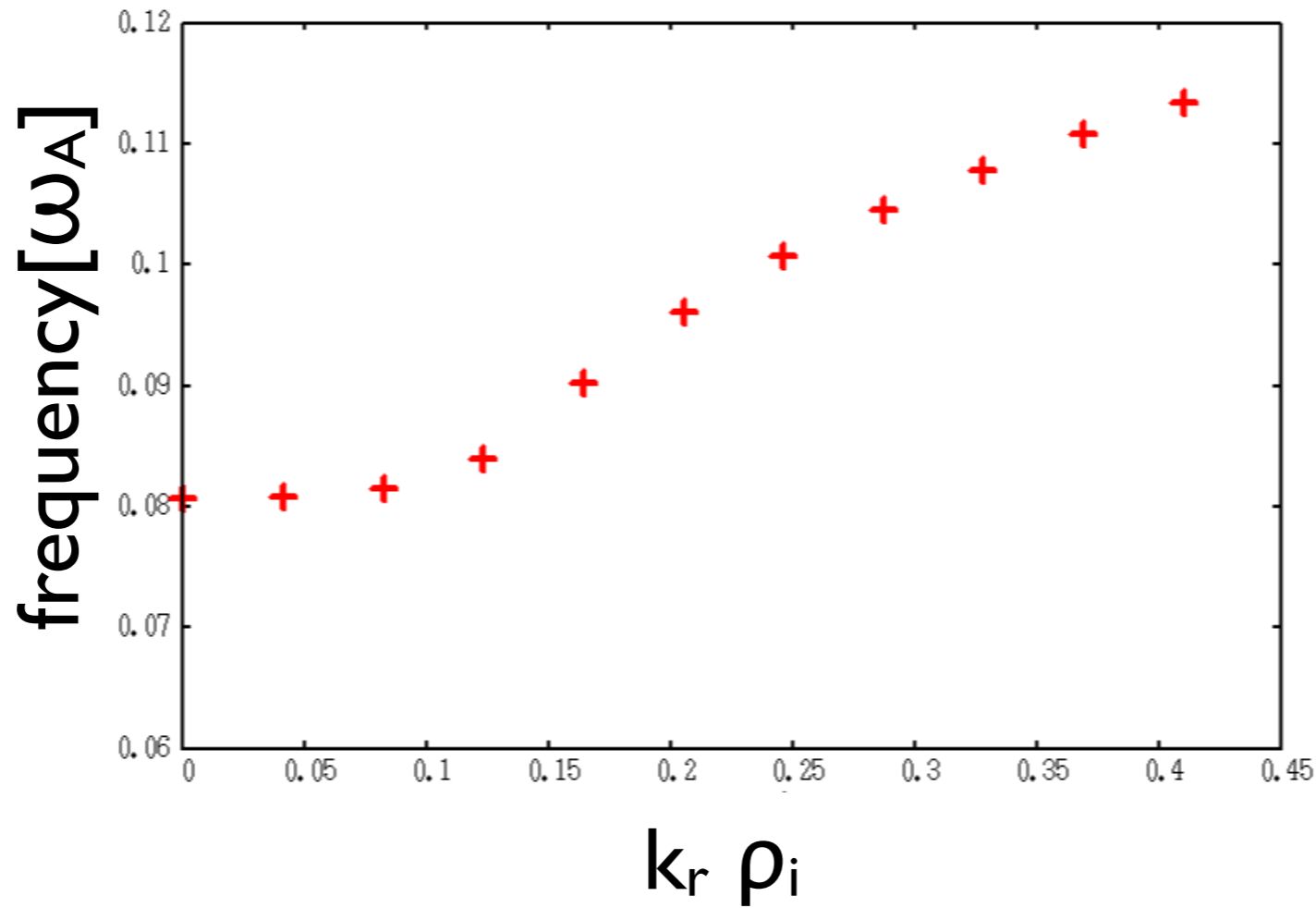
- analytical/numerical models point out importance of radial GAM/EGAM propagation [Zonca 2008, Qiu, 2009, Smolyakov 2009, Sasaki, Miki&Idomura 2015, Palermo 2017, etc..]
- nonlinear simulations GYSELA, GTS [Zarzoso, Schneller] and nl-analytical models [Sasaki] emphasise the role of radial GAM/EGAM propagation for turbulence spreading



[Schneller, 2017  
MPPC meeting;  
modified AUG]

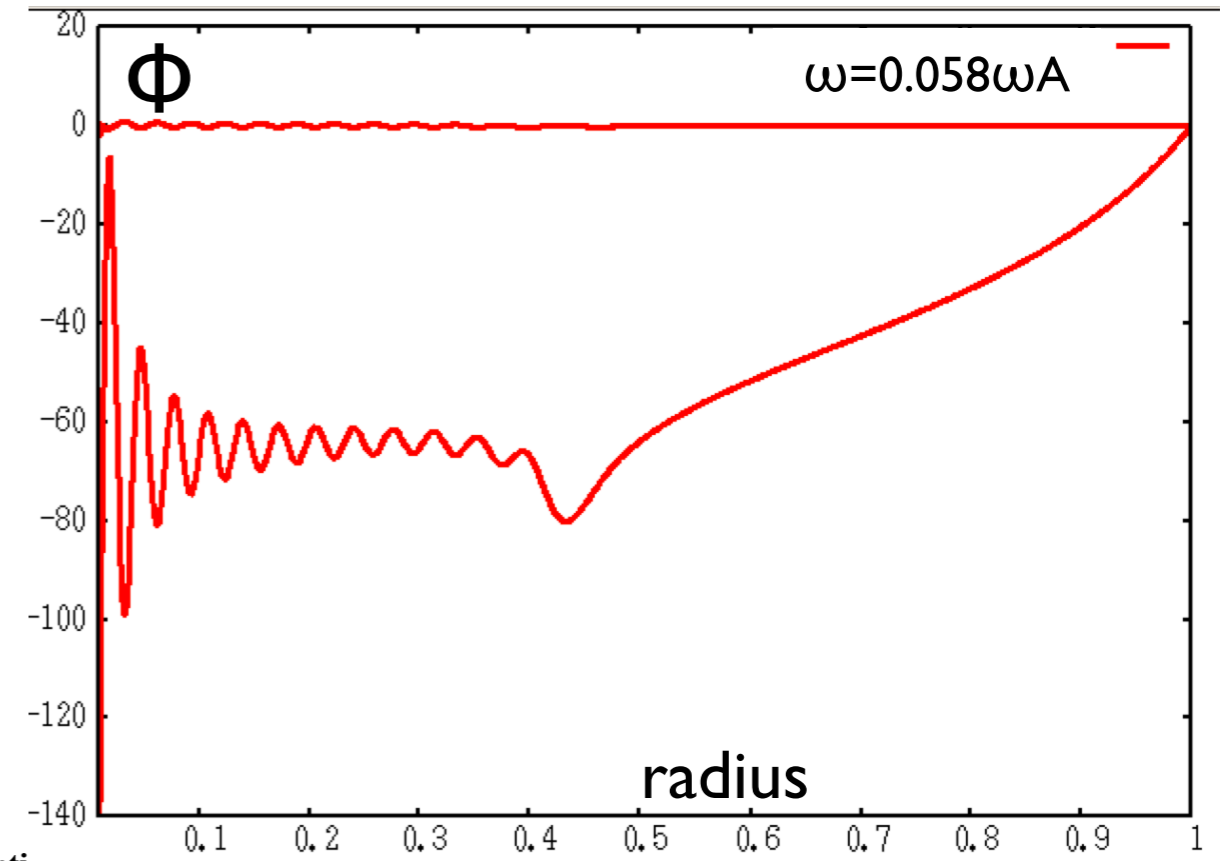
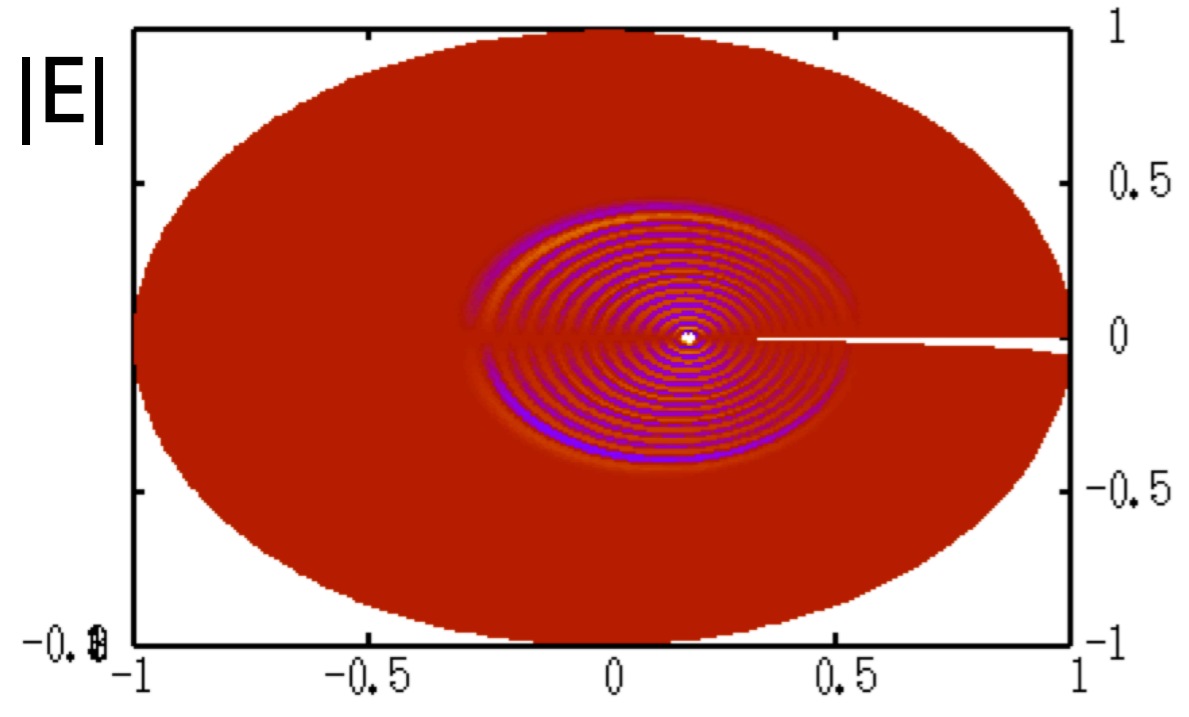
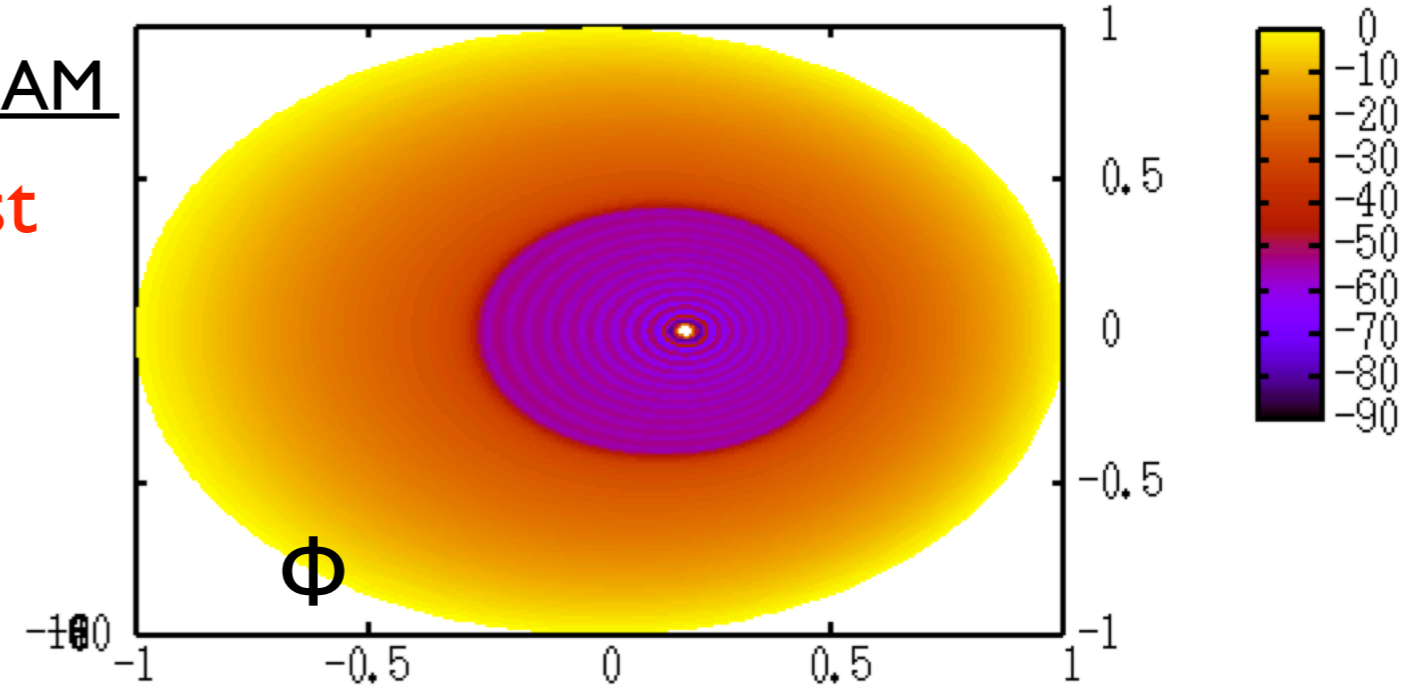
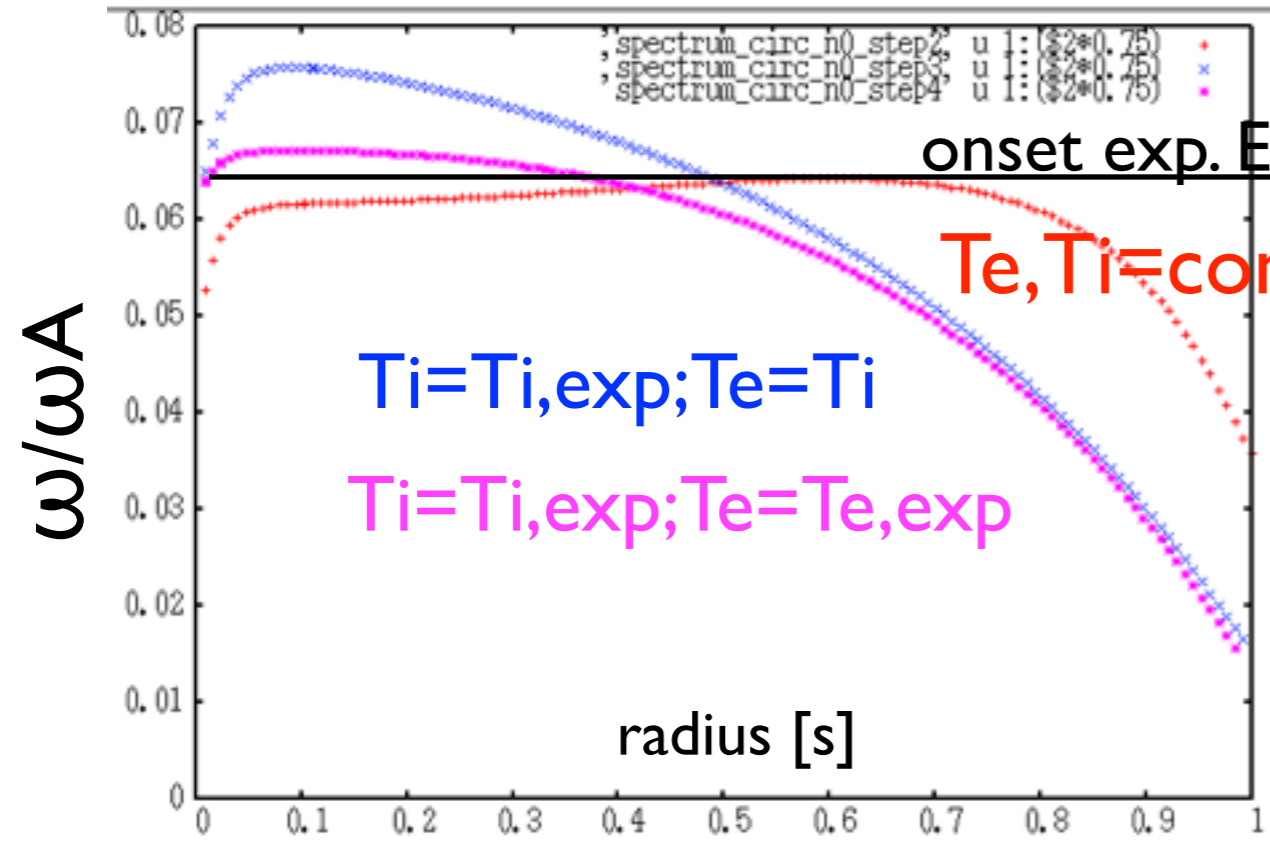
# newly developed FLR/FOW analytical LIGKA allows for radial propagation studies: $\omega(k_r)$

$v_g = \partial\omega/\partial k_r$  can be determined from this:



outward propagation for  $q=2.1$

# stable, global kGAM solutions emphasize importance of GAM continuum [LIGKA], exp. $f_{EGAM}$ close to $f_{GAM}$





# Effects of velocity anisotropy on the excitation of EGAMs;

*Work in progress; To be submitted to Nuclear Fusion: Conf. series ,  
I Chavdarovski, M Schneller, Z Qiu, A Biancalani;*

- The local dispersion relation of energetic -particle-induced Geodesic acoustic mode (EGAMs) is derived for both **circulating and trapped particle** beam with single pitch angle **slowing down and Maxwellian** distribution.
- Solutions of the local dispersion relation for each case give the **spectrum, the growth rate** and the threshold of excitation as function of the slowing down critical energy (for the trapped ) and the pitch angle (for circulating).
- Sample result: dispersion relation for trapped EP with slowing down distribution, as function of the **bounce frequency and  $\Lambda$** . The logarithmic term gives the drive.

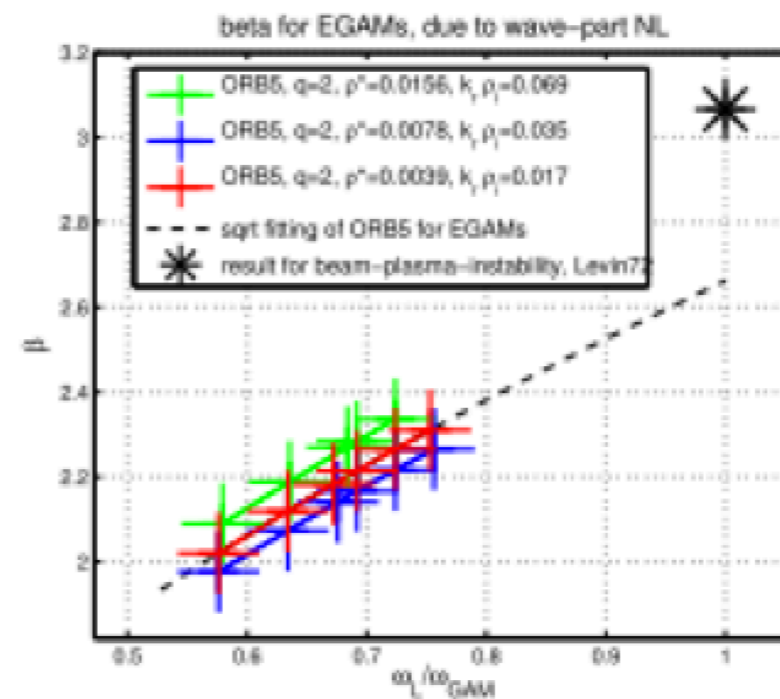
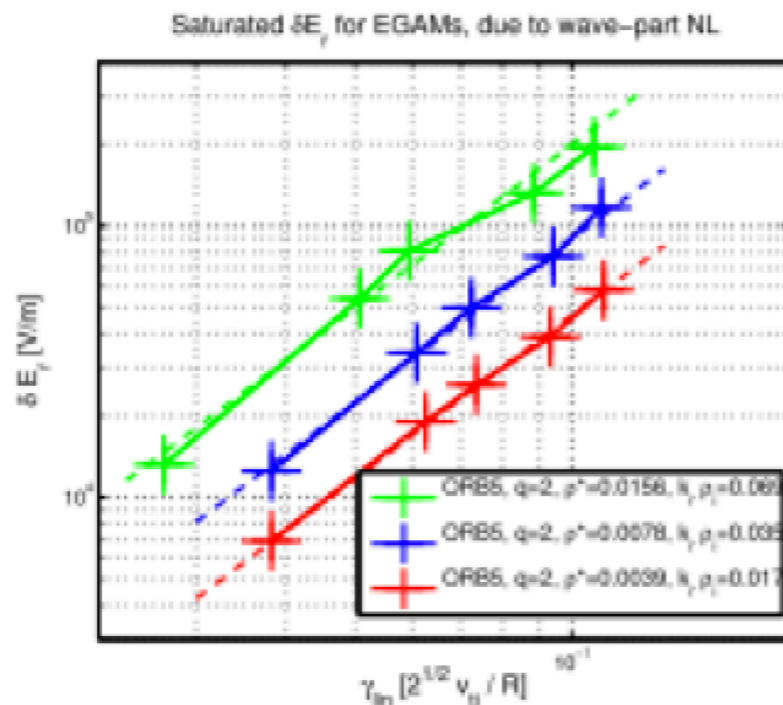
$$0 = -1 + \frac{\omega_G^2}{\omega^2} + \frac{\pi}{8} N_b \frac{1}{\epsilon \Lambda_0 B_0} \left[ \frac{3 - 2\Lambda_0 B_0 (1 - \epsilon)}{2(1 - \Lambda_0 B_0 (1 - \epsilon))^{3/2}} \log \left( 1 - \frac{\omega_b^2}{\omega^2} \right) + \frac{1}{1 - \Lambda_0 B_0 (1 - \epsilon)^{1/2}} \cdot \frac{\omega_b^2 / \omega^2}{1 - \omega_b^2 / \omega^2} \right]$$

to be implemented together with anisotropic shifted Maxwellian  
into LIGKA

# Saturation of EGAMs due to wave-particle nonlinearity

*Work by A Biancalani, I Chavdarovski and Z Qiu. Currently on IPP pinboard.*

- Only **wave-particle nonlinearities** are considered.
- The EGAM **saturates** mostly due to **flattening of the EP profile** in velocity space.
- **Quadratic scaling** of the saturated electric field with the linear growth rate is found, similarly to the beam-plasma instability:  $\delta \bar{E}_r = \alpha_2 \gamma_L^2$



# Non-linear generation of Zonal Flow and EGAMs second harmonic;

*Published work Z Qiu , I Chavdarovski, A Biancalani and J Cao,*

*Physics of Plasmas 24, 072509 (2017);*

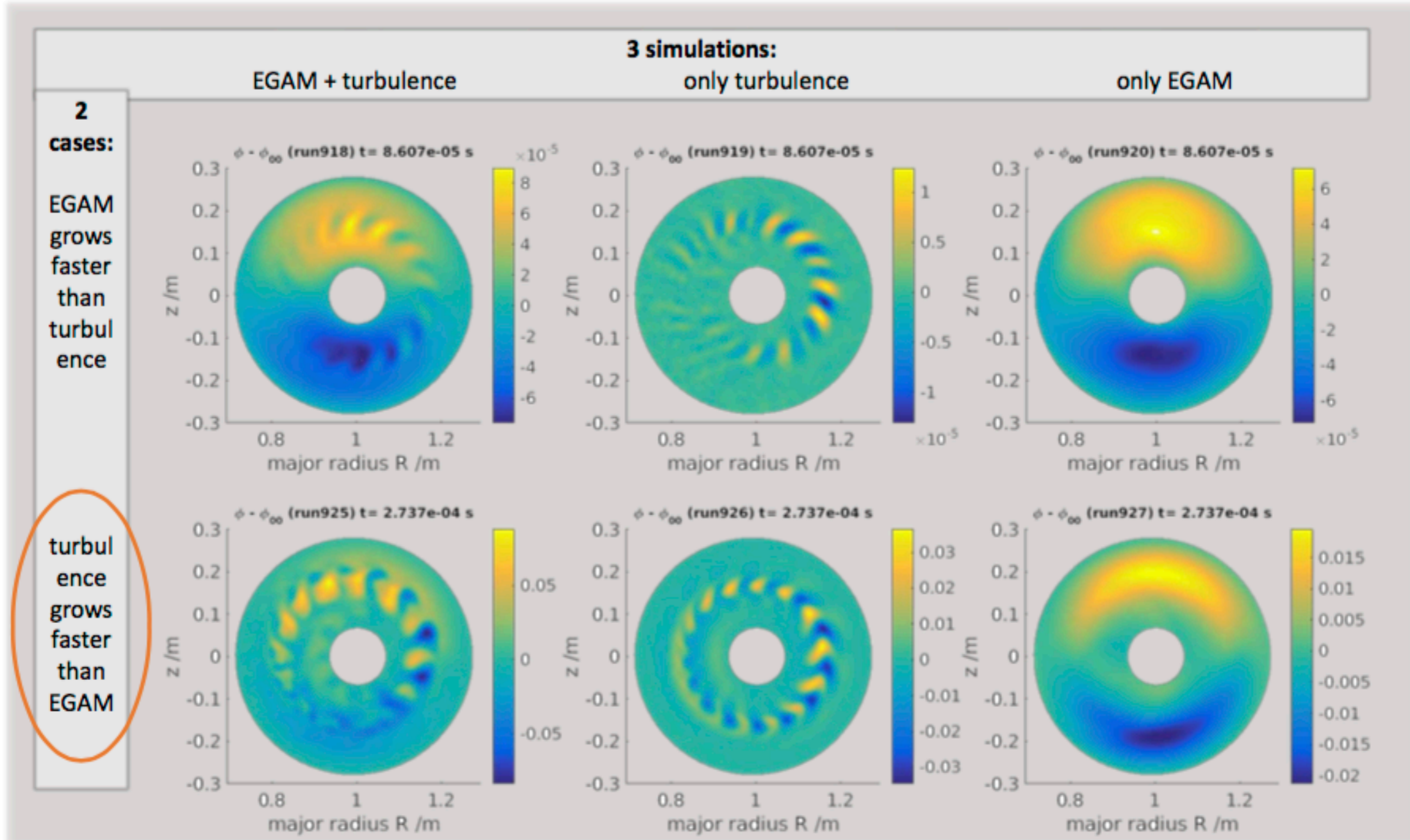
- Both second harmonic and ZFZFs can be driven by EGAMs, with the finite orbit width (FOW) effects playing a dominant role in the nonlinear couplings, contrary to the thermal where toroidicity dominates
- The contribution of resonant EPs to the cross-section of the nonlinear couplings dominates that of the thermal plasma.
- The generated ZFZF has a radial scale length half of the pump EGAM and growth rate double the size.
- For GAMs perpendicular and parallel non-linearities cancel out , but present EP will dominate (Fu 2011). Second harmonic is generated with  $l=1,2$  resonances and radial scale half of the primary EGAM.

$$b_S \hat{\mathcal{E}}_{EGAM}(\omega_S) \hat{\Phi}_S = -\frac{ik_r T_i}{n_0 m \Omega} \left\langle \frac{\partial F_{0h}}{\partial E} \frac{3\omega \hat{\omega}_d^2}{(\omega^2 - \omega_{tr}^2)(\omega_S^2 - \omega_{tr}^2)} \right\rangle \times \frac{\hat{\Phi}_G \hat{\Phi}_G}{r}$$

$$\hat{\mathcal{E}}_{EGAM}(\omega_S) \equiv -1 + \frac{\omega_G^2}{\omega_S^2} + \frac{T_i}{n_0 m_i b_S} \left\langle \frac{\partial F_{0h}}{\partial E} \sum_{l=\pm 1, \pm 2} \frac{J_l^2(\hat{\Lambda}_S) \omega_S}{\omega_S - l\omega_{tr}} \right\rangle$$

[M Schneller, MPPC 2017]

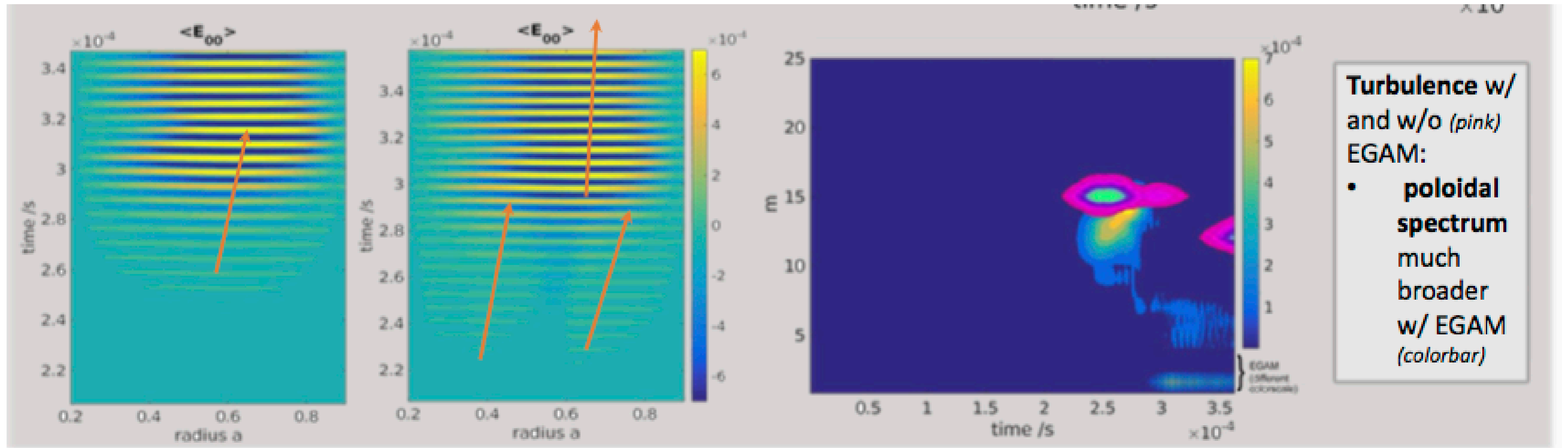
## 5. Study Case for EGAM & Turbulence Investigation



EGAM grows faster than turbulence

turbulence grows faster than EGAM

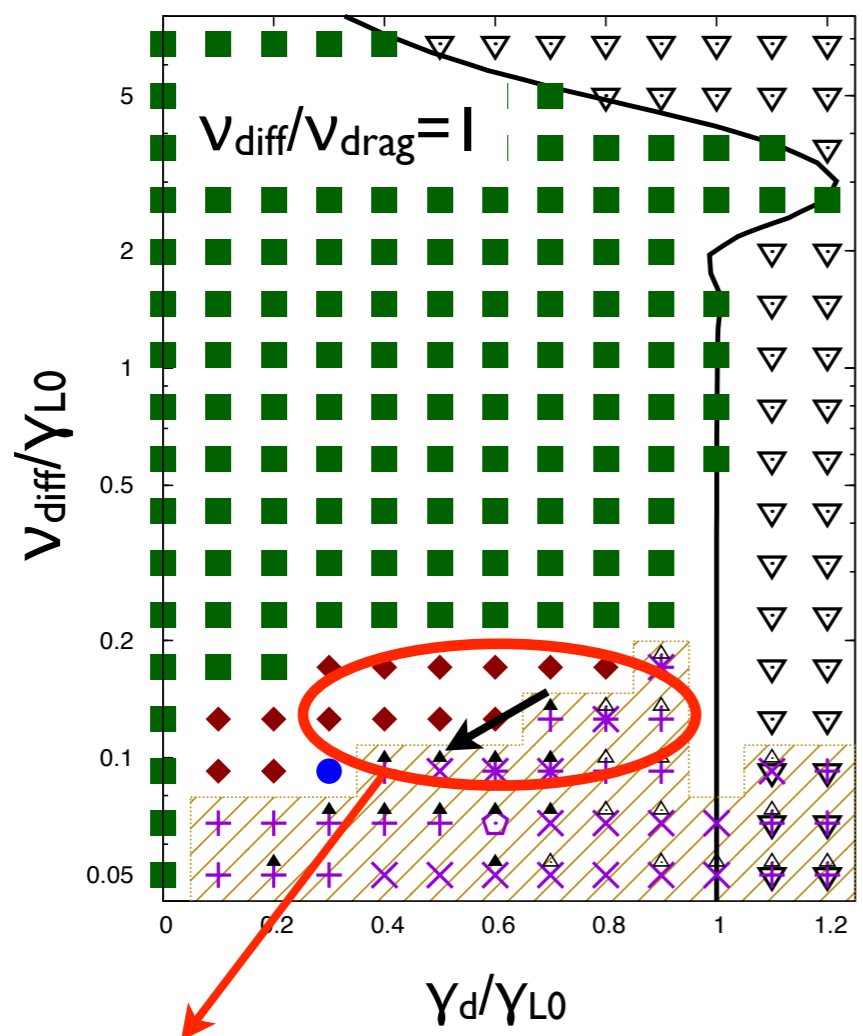
radial propagation and mode localisation changes in EGAM+turbulence case, more complex than in Zarzoso[2015], Sasaki[2017]



modelling to be continued step by step  
comparison of analytical theory, linear and non-linear simulations  
with experiments ongoing

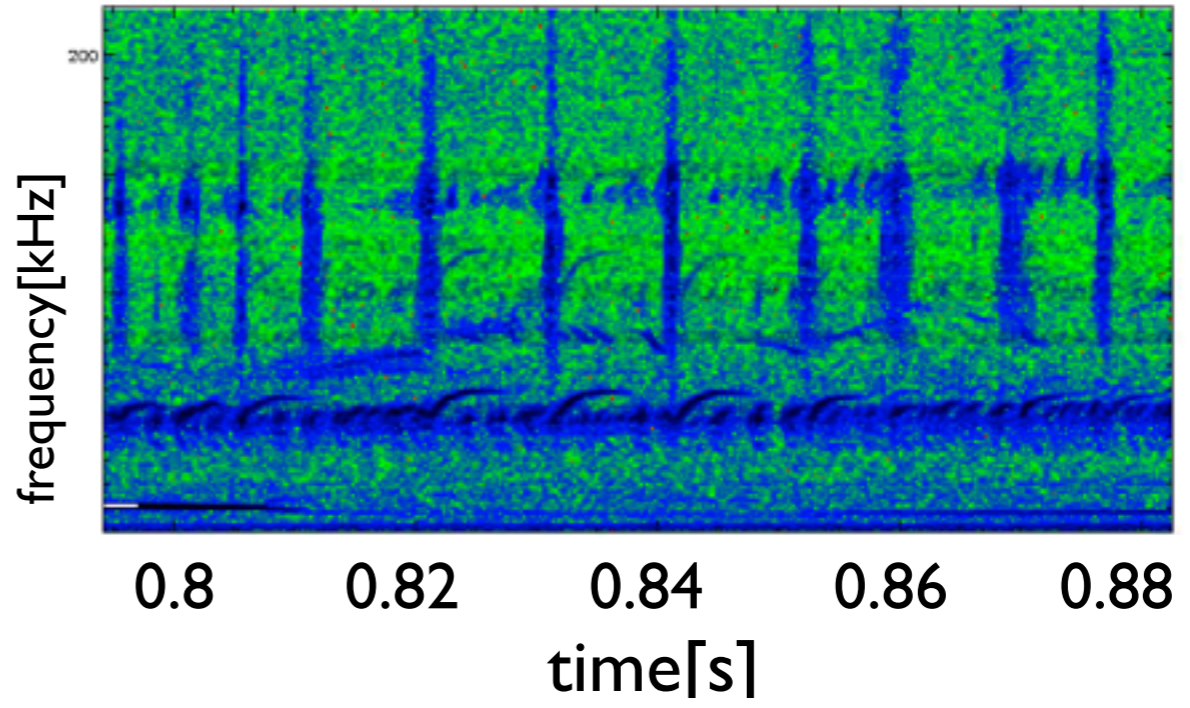
new discharge proposals (~#8-10):

- slightly reduce current to prolong stable  $q \sim 2$  phase:  
determine importance of AEs/EGAM and  $q=2$  crashes with respect to EP transport (maybe also ECCD necessary)
- attempt elongation scan in flat top
- add ECRH for threshold studies
- add ICRF for impact of drag/diffusion chirping



[M. Lesur, 2013]

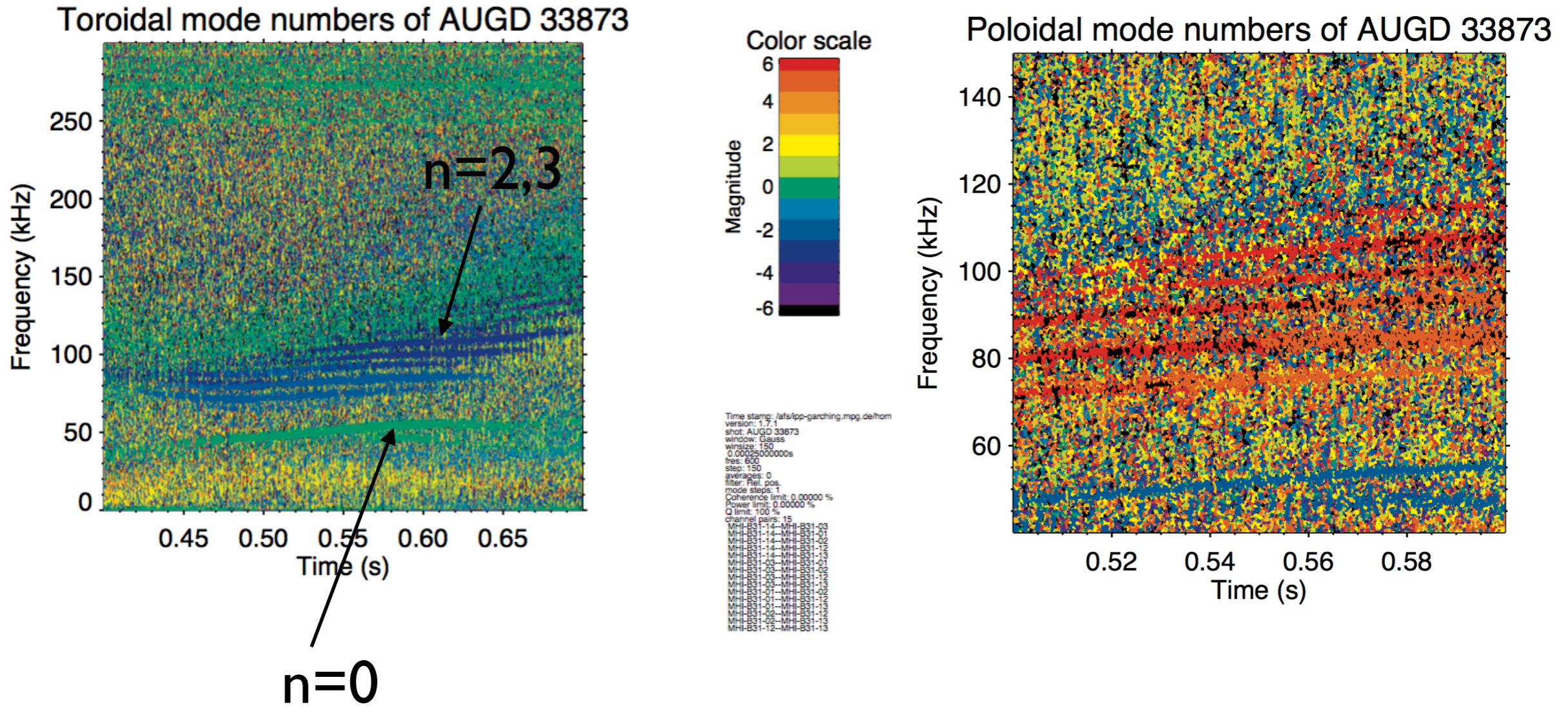
- Linear stability threshold —
- Steady-state threshold - - - -
- Steady/periodic threshold - · - · -
- Damped ▽
- Steady □
- Periodic ○
- Chaotic ◇
- Periodic chirping ⬠
- Bursty chirping +
- Intermittent chirping ×
- Chaotic chirping \*
- Steady hole ■
- Oscillatory hole ●
- Wavering hole ◆
- Upward chirping dominant ▲
- Downward chirping dominant ▼
- Upward chirping only ▲
- Downward chirping only ▼
- Hooked □



AUG? increased linear growth rate would explain transition from 'wavering hole' to hooked up-chirping

or low level of turbulence?

for higher B: multiple TAEs with the same n and m!



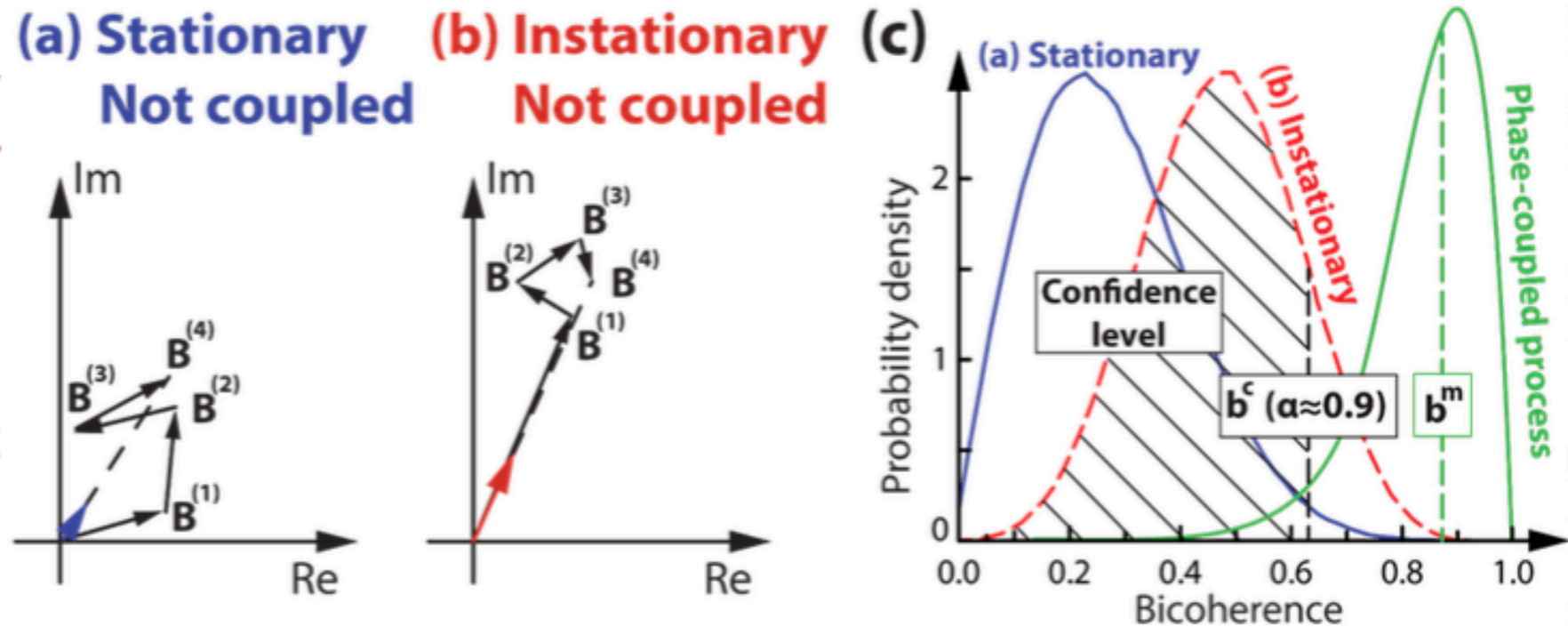
instability threshold for EGAM clearly observed,  
no chirping



- **Bicoherence analysis** is a widely applied method for identifying quadratic nonlinear interactions of **stationary processes** [1]

$$b^2(f_1, f_2) = \frac{|\mathbf{A}[X(f_1)X(f_2)X^*(f_1+f_2)]|^2}{\mathbf{A}[|X(f_1)X(f_2)|^2]\mathbf{A}[|X^*(f_1+f_2)|^2]}, \text{ with } \mathbf{A}[Y] := \lim_{N \rightarrow \infty} \frac{1}{N} \sum_{i=1}^N Y_i,$$

- Signals exhibiting **rapidly changing amplitudes or frequencies** (typical in the case of strongly driven EPMs) may cause **high bicoherence even without phase coupling**



- **Phase randomized bicoherence probability density function** calculation for each  $(f_1, f_2)$  point, which will **describe** a random **process without any phase coupling**.

- We can set an  **$\alpha$  confidence level**, which will define a  **$b_c$  critical bicoherence value** (at each  $(f_1, f_2)$  point)

$$\alpha = \int_0^{b^c} \rho(b) db$$

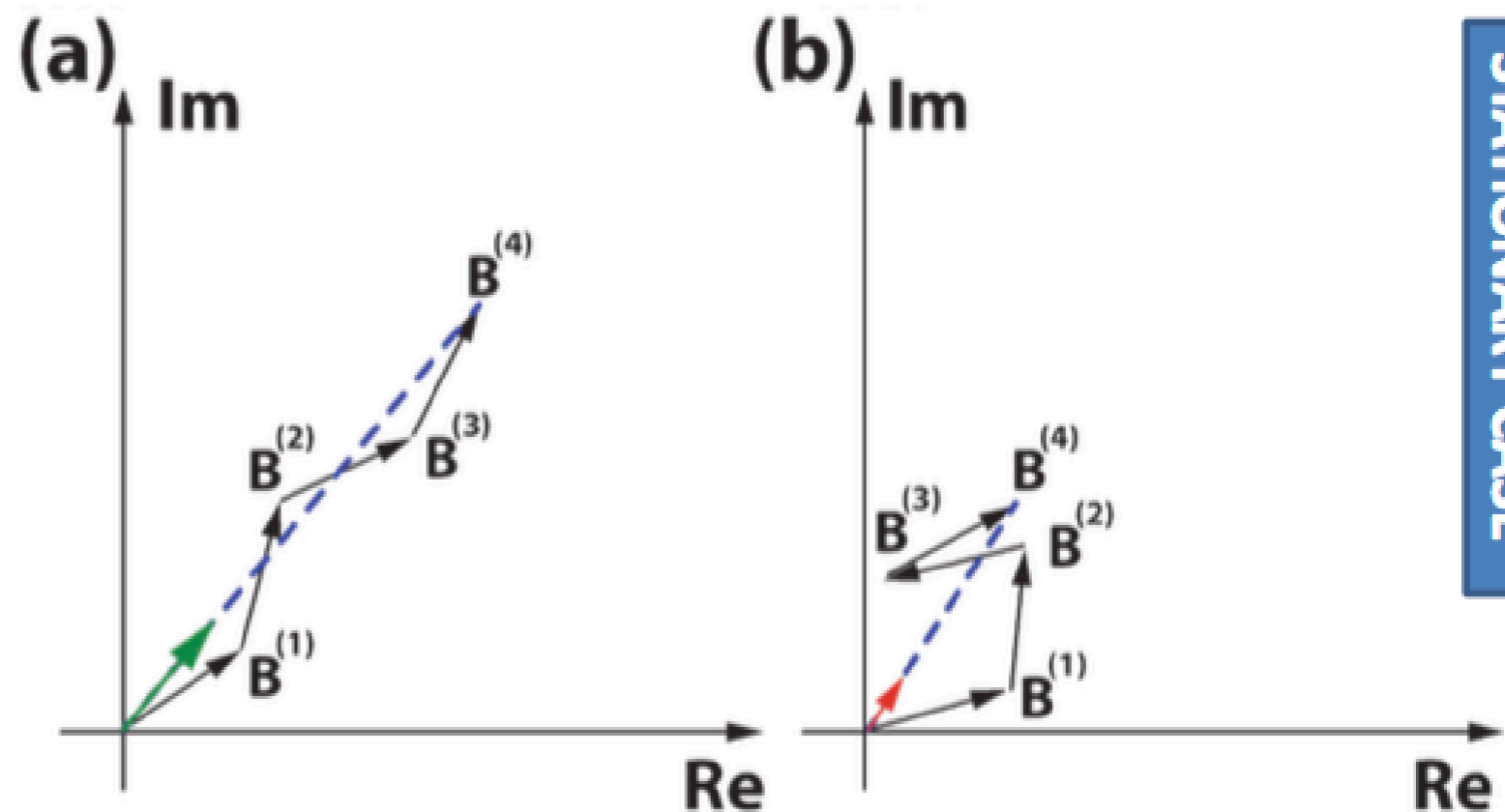
- **Bicoherence values higher than  $b_c$**  are from **non-phase coupled** process with  **$1-\alpha$  probability**. **Confidence level** can be used as a **filtering parameter**, by only plotting bicoherence values higher than  $b_c$ , thus **eliminating probable false positives**

# Bicoherence for stationary processes

- Used for detecting quadratic nonlinearities

$$B(f_1, f_2) = \mathbb{E} [X(f_1)X(f_2)X^*(f_1 + f_2)]$$

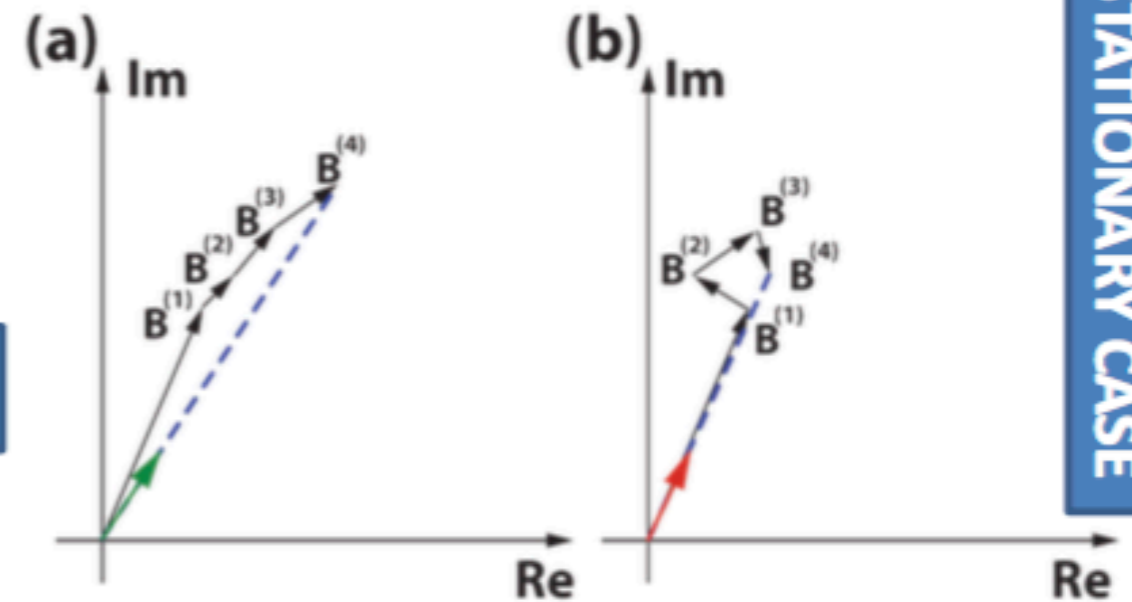
- Bispectrum calculation as random walk on the complex plane



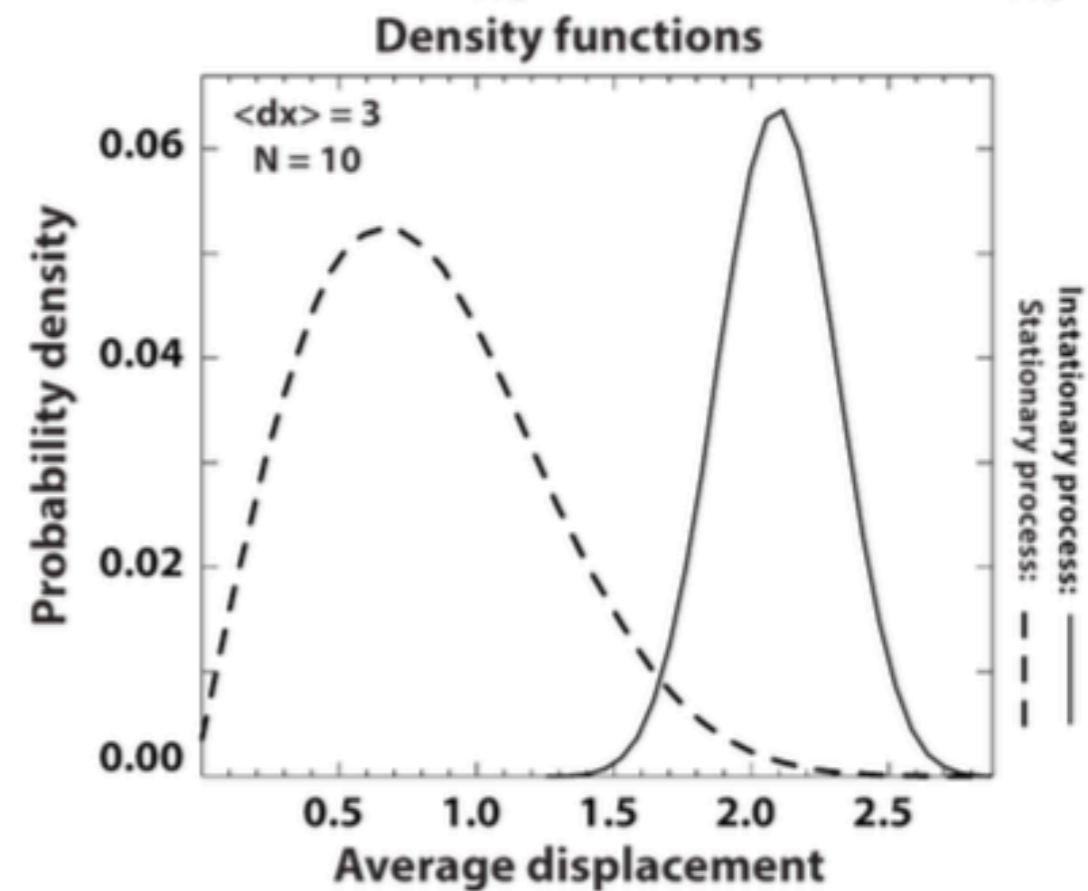
STATIONARY CASE

# Bicoherence for instationary case

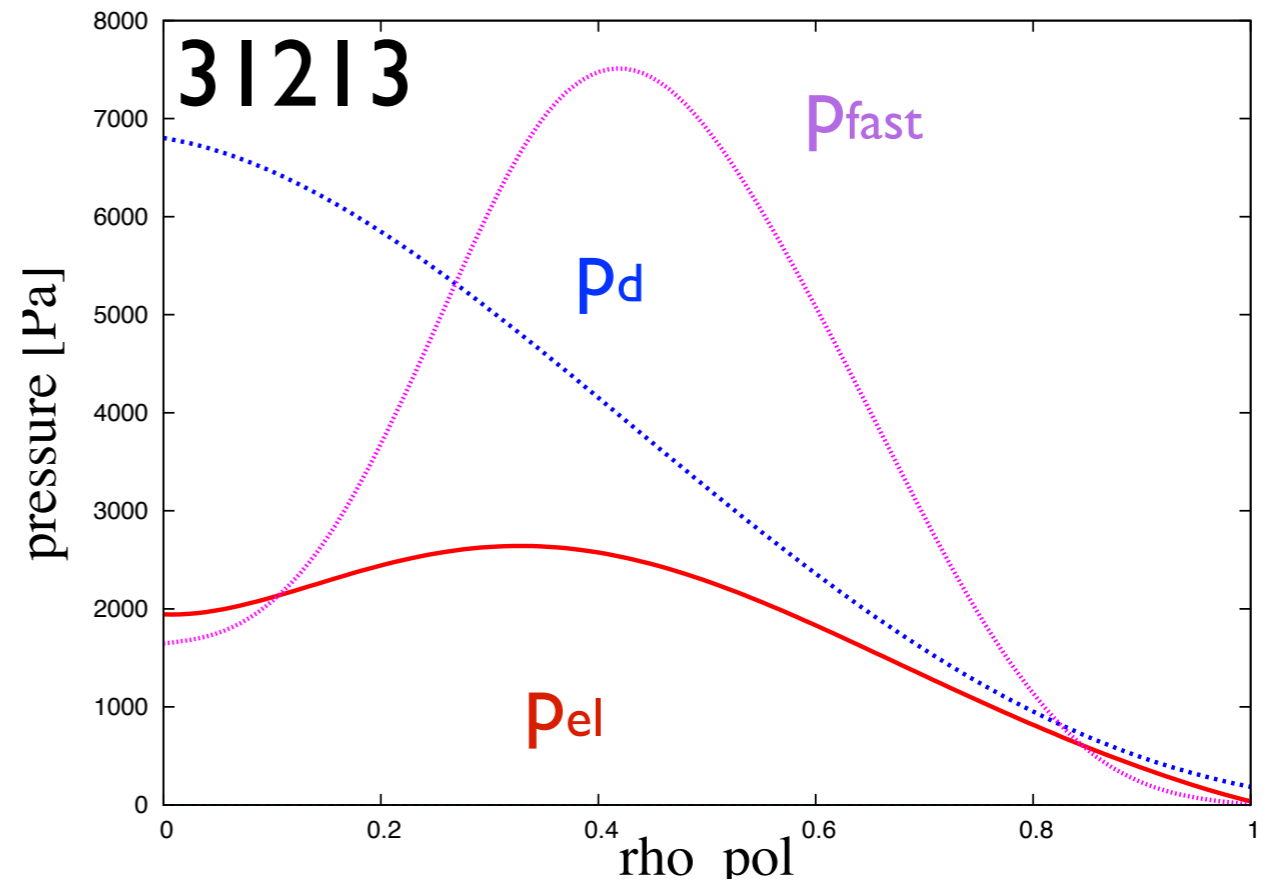
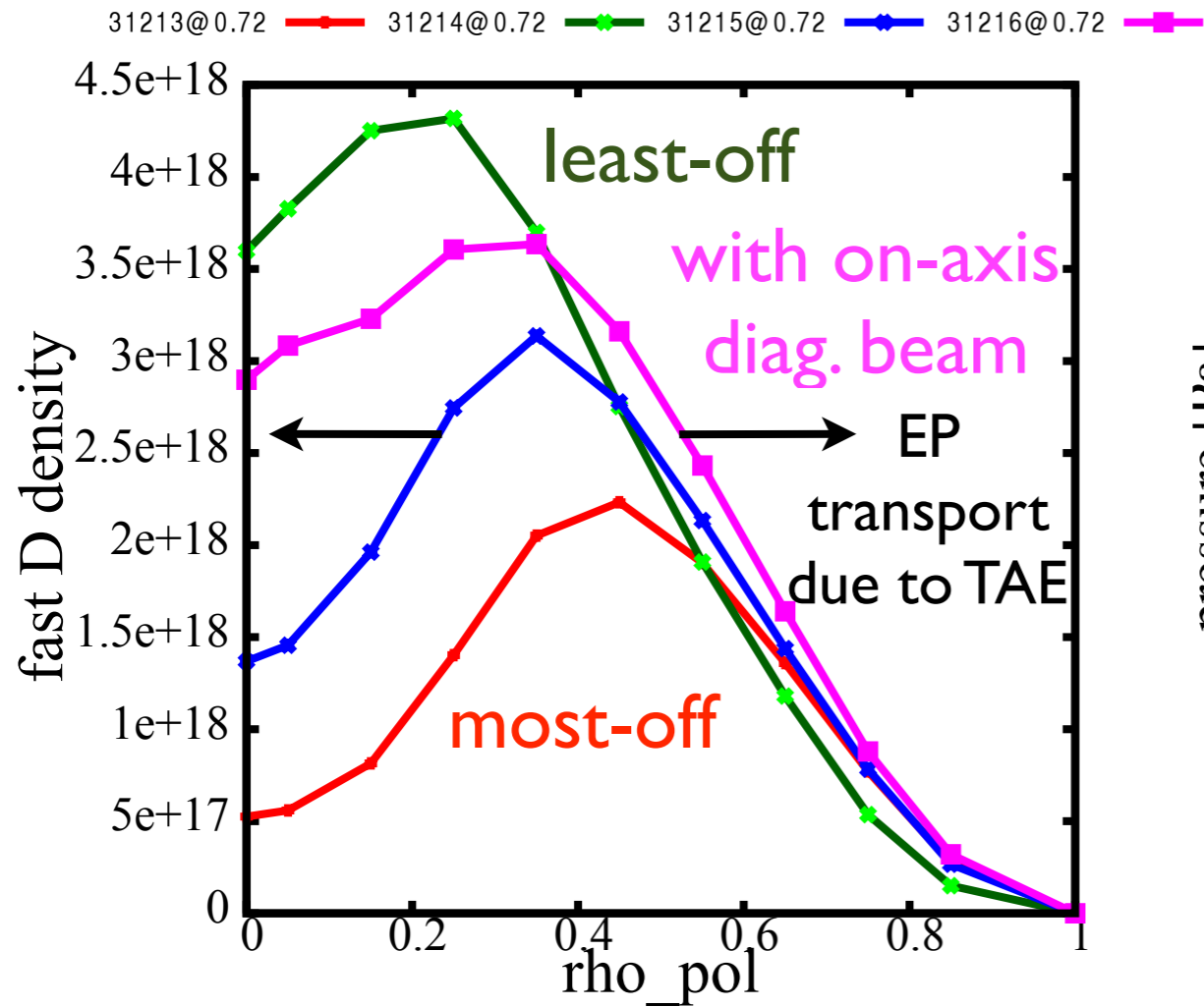
- Due to instationarity „false high” bicoherence
- Random walk with same total length, but different step length
- Significant differences in the probability density functions of bispectrum



INSTATIONARY CASE



#	EGAM/BAE/	NBI	angle	behav	later heating	I	B
27923	y/y/y/n	2:0.35-0.5;3:0.38-0.59;80.59-0.63;5:0.63-0.76;7:0.76	6,65				
28880	n/y/y/n	2:0.35-0.5;3:0.5-0.6;7:0.6	6,65			I	2.4
28881	y/y/y/n	2:0.35-0.5;3:0.5-0.6;7:0.6	6,65			I	2.4
28883	n/y/n/n	2:0.35-0.5;3:0.5-0.6;7:0.6	6,65				ASDEX Upgrade
28884	y/y/y/n	3:0.5-0.6;7:0.6	6,65			I	2,4
28885	y/y/y/n	2:0.35-0.5;3:0.5-0.6;7:0.6	6,65			I	2,4
30383	y/y/y/n	7: 0.26-0.75	6,65	Hmode		I	2,6
30945	n/y/n/n	2:0.28-0.376;6:0.382-0.697	6,65	dis@4s		I	2,2
30946	y/y/n/y	2:0.28-0.445;6:0.451-0.928	6,65	Lmode	no heating!	I	2,2
30947	y/n/n/y	2:0.28-0.478;6:0.482-0.928	6,65	dis@4s	H mode	I	2,2
30948	n/y/y/n	2:0.28-0.491;3:0.497-0.789	6,65	dis@1.2s	Q6@0.789	I	2,2
30949	y/y/n/n	2:0.35-0.5;3:0.38-0.79;6:0.79;7:1.0;8:1.2	6,65	dis@1.5		I	2,2
30950	y/y/y/n	3:0.28-0.295;7:0.312-0.797	6,65	dis@1.5	3:0.8-0.92;6.8@0.9	I	2,2
30951	n/y/n/n	3:0.28-0.295;5:0.312-0.552,8	6,65	dis@1.7	8-0.84;3:-0.99	I	2,2
30952	y/y/y/n	3:0.28-0.295;7:0.312-0.797	6,65	dis@1.18	Q6@0.8	I	2,2
30953	y/y/n/n	3:0.28-0.295;6:0.312-0.753	6,65	dis@1.11	Q2@0.76++	I	2,2
31213	y/y/y/n	3:0.28-0.295;7:0.296-1.033	7,13	dis@1.7	Q6@1.0	I	2,2
31214	y/y/y/n	3:0.28-0.295;7:0.296-1.033	6,05	dis@1.0		I	2,2
31215	y/y/y/n	3:0.28-0.295;7:0.296-1.033	6,65	dis@1.0		I	2,2
31216	y/y/y/n	3:0.28-0.295;7:0.296-3.045+blips	6,65	Lmode		I	2,2
31233	y/y/y/n	3:0.28-0.501;7:0.506-3.227	7,13	Hmode	Q6@1.0	I	2,2
31234	y/n/y/n	3:0.28-0.310;7:0.318-0.813	7,13	dis@ 0.8		I	2,2
32326	y/n/y/y	7: 0.28 +blips	7,13	EGAMS, TAEs		I	2,2
32327	y/n/y/n	7: 0.28 +blips: 82kV	7,13	transition		I	2,2
32328	n/n/n/n	7: 0.28 +blips +0.5 ECRH	7,13	only turbulence		I	2,2
32329	n/n/n/n	7: 0.28 + blips+0.5 ECRH	7,13	only Alfvénic turb		I	2,2
32384	y/n/y/n	7: 0.28 +blips 93kV	7,13	too high density		I	2,2
32386	y/n/n/n	7: 0.28 +blips: 65kV	7,13			I	2,2
32387	y/n/y/y	7+6: 0.28 +blips: 65kV	7,13			I	2,2
32388	y/y/y/y	7: 0.28 +blips + higher density 93kV	7,13			I	2,2
33872	y/y/y/y	7: 0.28 +blips + higher density 93kV	7,13		diff breakdown		no Te inversion 2.2
33873	y/y/y/y	7: 0.28 +blips + higher density 93kV	7,13		diff breakdown		no Te inversion 2.5
33874	y/y/y/y	7: 0.28 +blips + higher density 93kV	7,13	dis@1.0	std brkdwn		no Te inversion 2.0
33875	y/y/y/y	7: 0.28 +blips + higher density 93kV	7,13	dis@1.0s	std brkdwn		no Te inversion 2.2
34184	y/y/y/y	7: 0.28 +blips + higher density 93kV	7,13	shape scan t>0.8			Te inversion 2.2
34185	y/y/y/y	7: 0.28 +blips + higher density 93kV	7,13	shape scan t>0.8			Te inversion 2.2
34186	y/y/y/y	7: 0.28 +blips + higher density 93kV	7,13	std			Te inversion 2.2
34187	y/y/y/y	7: 0.28 +blips + higher density 93kV	6,65	std			Te inversion 2.2

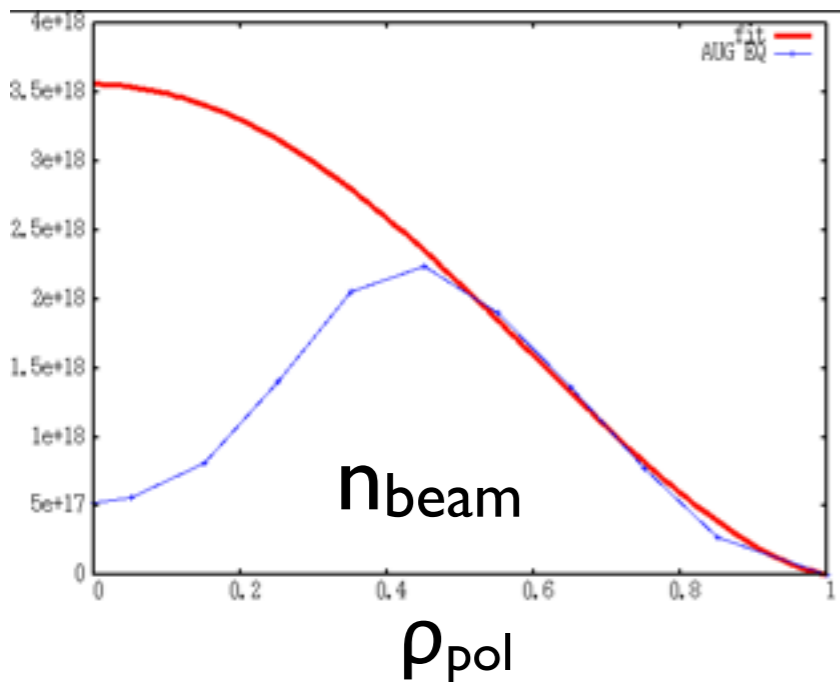
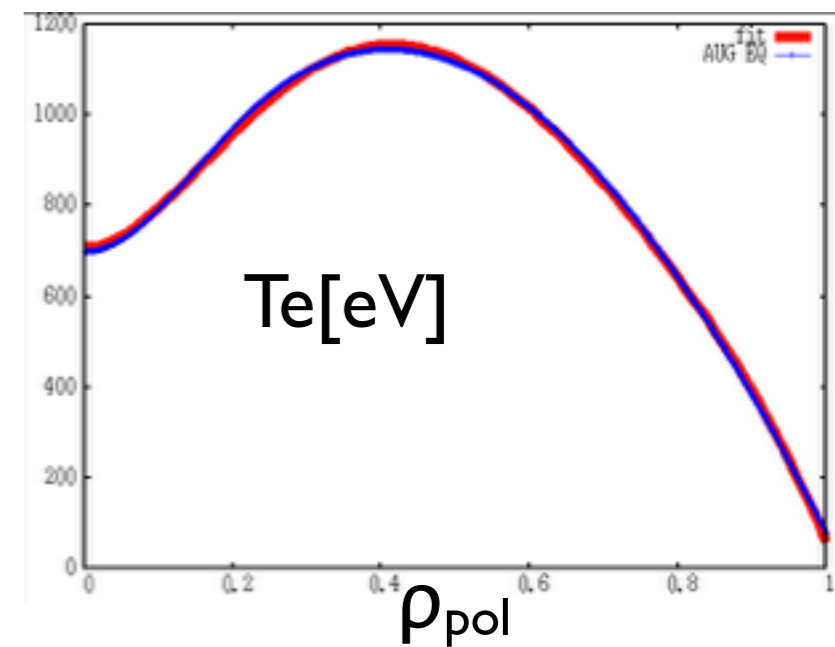
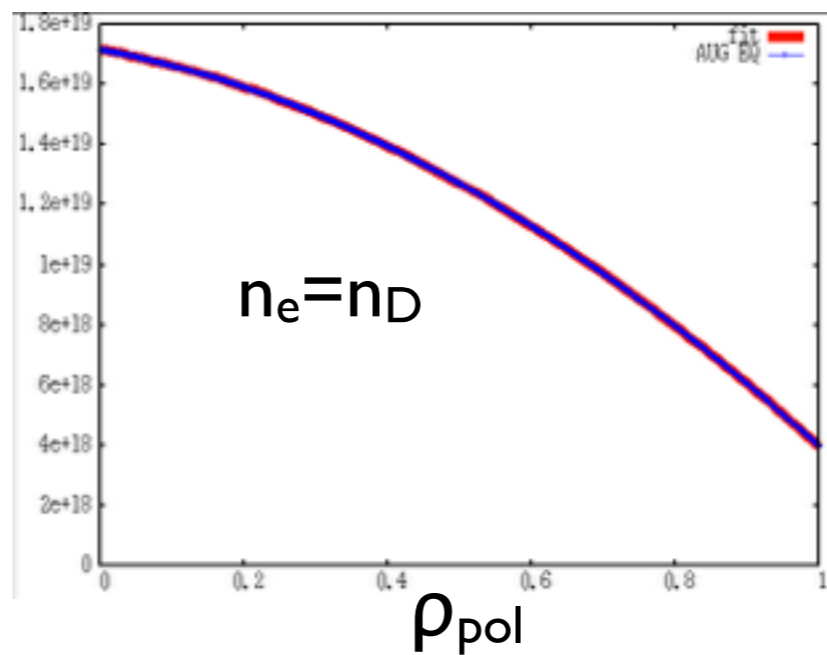
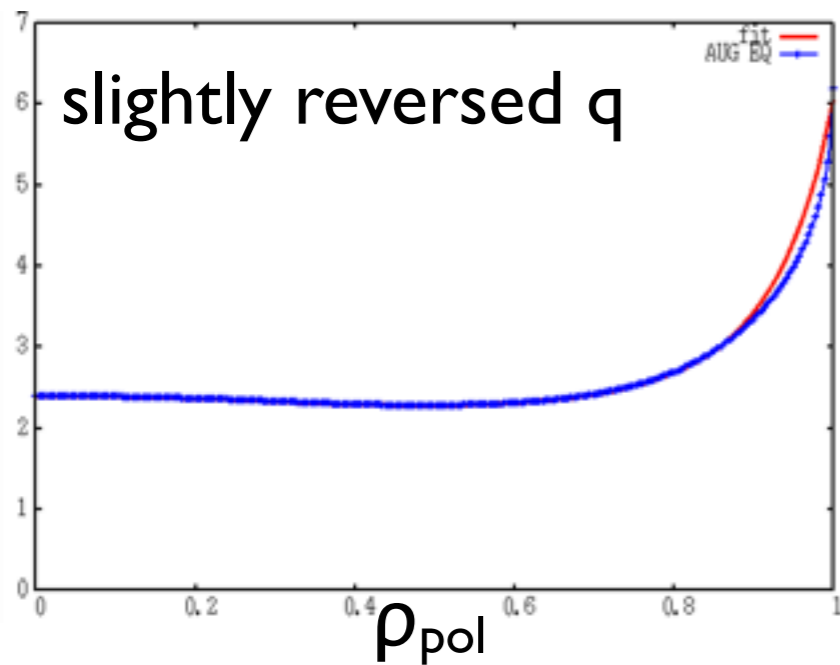


$$p_{EP} \approx p_e + p_d$$

$$\beta_{EP} / \beta_{th} > 1; T_f \sim 90 T_i$$

DEMO-like conditions for these two parameters

[http://www2.ipp.mpg.de/~pwl/NLED\\_AUG/data.html](http://www2.ipp.mpg.de/~pwl/NLED_AUG/data.html)



benchmark  
 steps:  
 step 1: flat  $T_e, T_i, n_e$   
 step 2:  $n_e$ , flat  $T_e, T_i$   
 step 3:  $n_e, T_e = T_i$   
 step 4:  $n_e, T_e \neq T_i$

